Structural and Multidisciplinary Optimization (2019) 60:1035–1058
https://doi.org/10.1007/s00158-019-02255-1

RESEARCH PAPER

Reliability-based topology optimization by ground structure method employing a discrete filtering technique

Junho Chun[1] · Glaucio H. Paulino[2] · Junho Song[3]

Received: 5 September 2017 / Revised: 13 February 2019 / Accepted: 5 March 2019 / Published online: 16 June 2019
© Springer-Verlag GmbH Germany, part of Springer Nature 2019

Abstract

When conventional filtering schemes are used in reliability-based topology optimization (RBTO), identified solutions may violate probabilistic constraints and/or global equilibrium. In order to address this issue, this paper proposes to incorporate a discrete filtering technique termed the discrete filtering method (Ramos Jr. and Paulino 2016) into RBTO using the elastic formulation of the ground structure method. The discrete filtering method allows the optimizer to achieve more physically realizable truss designs in which thin bars are eliminated while ensuring global equilibrium. The method uses a potential-energy-based approach with Tikhonov regularization to solve the singular system of equations that may result from imposing the discrete filter. Combining this method with RBTO allows us to use the reliability-based truss sizing optimization for the purpose of topology optimization under uncertainties. Furthermore, a single-loop approach is adopted to enhance the computational efficiency of the proposed RBTO method. Numerical examples of two- and three-dimensional engineering designs demonstrate useful features of the proposed method and illustrate the influence of the discrete filter and parameter uncertainties on the optimization results. In order to check if the optimal topologies obtained by the proposed approach satisfy the constraints on the failure probabilities, structural reliability analysis is also performed using the first-order reliability method and Monte Carlo simulations.

Keywords Reliability-based topology optimization · Ground structure · Single-loop approach · Discrete filtering

1 Introduction

Topology optimization is a computational-simulation-based tool which has been utilized to identify optimal topology solutions for various engineering problems. In particular, topology optimization of *continuum* structures seeks for optimal material layouts and connectivities in a given design domain (Bendsøe and Sigmund 2003). In such continuum-based topology optimization, the design domain is discretized with finite elements (or other methods), each of which is assigned to void or solid material through an iterative optimization procedure (see Rozvany (2009), and Deaton and Grandhi (2014) for a state-of-the-art review of topology optimization). In the field of structural engineering, continuum-based topology optimization has been applied to aid the design process of lateral-load resisting systems (Mijar et al. 1998; Stromberg et al. 2012; Bobby et al. 2014; Chun et al. 2016). On the other hand, topology optimization of *discrete* structures, such as trusses and frames, has been applied to find optimal connectivity of the nodes by the structural elements. This approach commonly implements the ground structure method (Bendsøe and Sigmund 2003; Ohsaki 2010), in which the design domain is discretized by use of spatial nodes, which are highly interconnected by either truss or frame elements. Topology optimization is performed on the generated ground structure to minimize the objective function while satisfying constraints, and thus the size of elements and connectivities are subsequently determined. Zegard and Paulino (2014, 2015) developed both two- and three-dimensional implementations of ground structure based topology optimization for trusses using the optimization for trusses using the so-called plastic formulation. The developed computer codes, GRAND and GRAND3, include an efficient algorithm for ground structure generation using restriction zones that allow

Responsible Editor: Xu Guo

✉ Junho Chun
jchun04@syr.edu

[1] School of Architecture, Syracuse University, Syracuse, NY, USA

[2] School of Civil and Environmental Engineering, Georgia Institute of Technology, Atlanta, GA, USA

[3] Department of Civil and Environmental Engineering, Seoul National University, Seoul, South Korea

for ground structure generation on arbitrary domains. Furthermore, topology optimization of truss structures considering an integrated discrete filtering was proposed by Ramos Jr. and Paulino (2016).

In the last decades, *deterministic* topology optimization (DTO) has been well developed for both continuum and discrete topology optimization. These methods consider all design parameters such as material properties, loadings, and geometry as deterministic quantities during the optimization. However, consideration of uncertainties in loads and material properties is critical in engineering efforts to manage the risk of unexpected structural failures that may eventually result in catastrophic damage. Therefore, optimization processes should utilize systematic treatment of uncertainties to obtain engineering solutions achieving a satisfactory level of reliability. This is widely referred to as reliability-based design optimization (RBDO; Frangopol and Maute 2005; Tsompanakis et al. 2008) or reliability-based topology optimization (RBTO; Maute and Frangopol 2003; Guest and Igusa 2008; Rozvany 2008). In particular, Nguyen (2010) proposed a system reliability-based design optimization using the matrix-based system reliability (MSR) method, which can consider statistical dependence and compute parametric sensitivity in an efficient way. This approach was further applied to the continuum topology optimization (Nguyen et al. 2011). Jalalpour et al. (2013) focused on the reliability-based topology optimization of a truss structure to address geometric imperfections and uncertainty in the material property.

Traditional formulations in RBDO and RBTO employ two nested loops of iterative computations: an optimization loop and a reliability analysis loop. The inner loop for reliability analysis is to evaluate probabilistic constraints or objective functions for the design variables updated by the outer loop for optimization. The solutions of reliability problems can be obtained by means of the First-Order Reliability Method (FORM) or the Second-Order Reliability Method (SORM) (see Der Kiureghian 2005 for a comprehensive review). To reduce computational cost in RBDO and RBTO, a single-loop approach has been developed (Du and Chen 2004; Liang et al. 2004, 2007, 2008; Shan and Wang 2008; Nguyen 2010). This method replaces the inner loop of the reliability analysis by an approximate non-iterative solution, which eventually tends to converge to an accurate reliability estimate as the optimal design is achieved through iterations.

In topology optimization for truss structures, a lower bound of design variables is set to a very small value to avoid an ill-posed condition such as a singular matrix. As a result, the converged topology still includes the original connectivity from the generated ground structure. To define the final topology, the conventional topology optimization for truss structures implements a filtering procedure at the end of optimization. More specifically, conventional filtering schemes select bars having areas greater than a small arbitrarily assigned cut-off value of the area, which subsequently become the bars defining the final optimized topology. However, the selection criteria for the lower bound and the cut-off are often ambiguous (Christensen and Klarbring 2009). Thus, conventional filtering methods may produce ill-conditioned solutions, such as a singular stiffness matrix, hanging members or many thin bars, which may be undesirable in engineering and architecture. Conventional filtering schemes in RBTO are thus highly likely to result in a final structure that violates not only the probabilistic constraints but also the global equilibrium condition. Therefore, development of a topology optimization framework for truss structures is needed to obtain reliable designs that satisfy global equilibrium and that are not dependent on the cut-off.

To address the aforementioned issues, a discrete filtering method proposed by Ramos Jr. and Paulino (2016) is incorporated into RBTO for truss structures in this paper so that more physically realizable truss designs are obtained, e.g., thin bars are eliminated while satisfying global equilibrium. As a result, by means of the proposed approach, a topology optimization problem under significant uncertainties can be solved effectively by the reliability-based truss sizing optimization. Moreover, the computational efficiency of the proposed method is further improved by utilizing a single-loop approach (Liang et al. 2004, 2007, 2008; Nguyen 2010).

2 Single-loop reliability-based topology optimization formulation

In this section, mathematical formulations of RBTO are first presented. Then, as a method to enhance computational efficiency in RBTO, a single-loop RBTO approach is reviewed. A study on concavity of probabilistic constraints is presented and effects of local and global optima in a lower level optimization problem, which is the inner loop for reliability analysis in RBTO, on a converged solution are discussed.

2.1 Reliability-based topology optimization

A general mathematical formulation of reliability-based topology optimization can be written as

$$\begin{aligned} \min_{\mathbf{d},\boldsymbol{\mu}_\mathbf{X}} \quad & f(\mathbf{d},\boldsymbol{\mu}_\mathbf{X}) \\ \text{s.t.} \quad & P[g(\mathbf{d},\mathbf{X})\le 0]\le {P_f}^{\text{target}} \\ & \mathbf{d}^{\text{lower}}\le\mathbf{d}\le\mathbf{d}^{\text{upper}} \\ \text{with } & \mathbf{K}(\mathbf{d},\mathbf{X})\mathbf{u}(\mathbf{d},\mathbf{X}) = \mathbf{f}(\mathbf{X}) \end{aligned} \tag{1}$$

where $f(\cdot)$ denotes the objective function, $\mathbf{d}$ represents the vector of design variables, and $\boldsymbol{\mu}_\mathbf{X}$ is the vector of the means of random variables in $\mathbf{X}$. $g(\cdot)$ is the limit-state function whose negative value indicates the violation of the given constraint. $P[\cdot]$ is the probability of the limit-state function $g(\cdot)\le 0$. $\mathbf{K}$, $\mathbf{u}$,

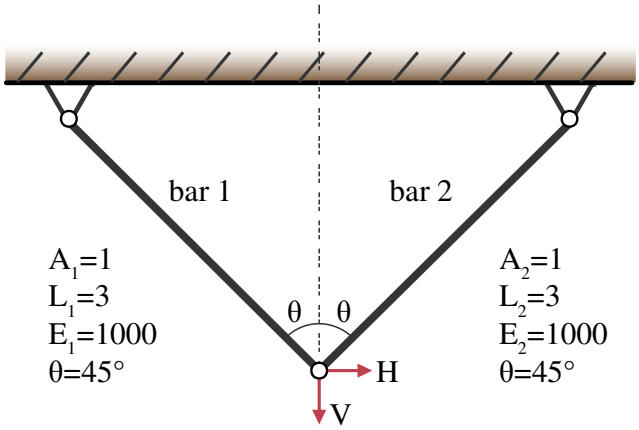

Fig. 1 Two-bar truss problem definition. Loading, boundary conditions, and material property

and **f** are the global stiffness matrix, the global displacement vector, and the global force vector, respectively. The probability of the failure event defined in terms of $g(\cdot)$ can be computed by integrating the joint probability density function (PDF) of **X** in the failure domain, i.e.

$$P = \int_{g(\mathbf{X})\le 0} f(\mathbf{x})d\mathbf{x} \tag{2}$$

By transforming the random variables to the space of uncorrelated standard normal random variables, i.e., $\mathbf{U} = \mathbf{T}(\mathbf{X})$ (Der Kiureghian 2005), the failure probability is given by

$$P = \int_{G(\mathbf{u})\le 0} \varphi_n(\mathbf{u};\mathbf{I})d\mathbf{u} \tag{3}$$

where **U** represents the vector of uncorrelated standard normal variables transformed from **X**. $G(\cdot)$ denotes the limit-state function given in terms of **U**, and $\varphi_n(\cdot)$ is the joint PDF of the n standard normal random variables. The correlation coefficient matrix of the joint PDF is given as the identity matrix **I** since the random variables are uncorrelated.

In general, RBTO consists of an outer loop for optimization and an inner loop for the reliability analysis. The reliability analysis forms a loop because reliability analysis methods such as the FORM or SORM (Der Kiureghian 2005) find the "most probable failure point (MPP)," $\mathbf{U}^*$ by performing constrained nonlinear optimization, i.e.

$$\mathbf{U}^* = \arg\min_{\mathbf{U}} \left\{ \|\mathbf{U}\| \mid G(\mathbf{d},\mathbf{U}) \le 0 \right\} \tag{4}$$

In the FORM, for example, the "reliability index" β in the standard normal space is obtained as

$$\beta = -\frac{\nabla G(\mathbf{U}^*)}{\|\nabla G(\mathbf{U}^*)\|}\cdot \mathbf{U}^* \tag{5}$$

Then, the failure probability in (3) is approximately evaluated by use of the reliability index β as

$$P \cong \Phi[-\beta] \tag{6}$$

where Φ is the cumulative distribution function (CDF) of the standard normal distribution.

Accordingly, the RBTO problem can be written using the so-called reliability index approach (RIA; Enevoldsen and Sorensen 1994) as follows:

$$\begin{aligned} &\min_{\mathbf{d},\boldsymbol{\mu}_\mathbf{X}} \quad f(\mathbf{d},\boldsymbol{\mu}_\mathbf{X}) \\ &\text{s.t.} \quad \beta(\mathbf{d},\mathbf{U}) \ge \beta^{\text{target}} \\ &\qquad \mathbf{d}^{\text{lower}} \le \mathbf{d} \le \mathbf{d}^{\text{upper}} \\ &\text{with } \mathbf{K}(\mathbf{d},\mathbf{X})\mathbf{u}(\mathbf{d},\mathbf{X}) = \mathbf{f}(\mathbf{X}) \end{aligned} \tag{7}$$

where $\beta^{\text{target}} = -\Phi^{-1}[P_f^{\text{target}}]$. Alternatively, the minimum value of the limit-state function on the surface of the hypersphere with the radius β^{target} can be used to check the violation of the probabilistic constraint. This is referred to as the performance measure approach (PMA; Tu et al. 1999). RBTO based on PMA is formulated as

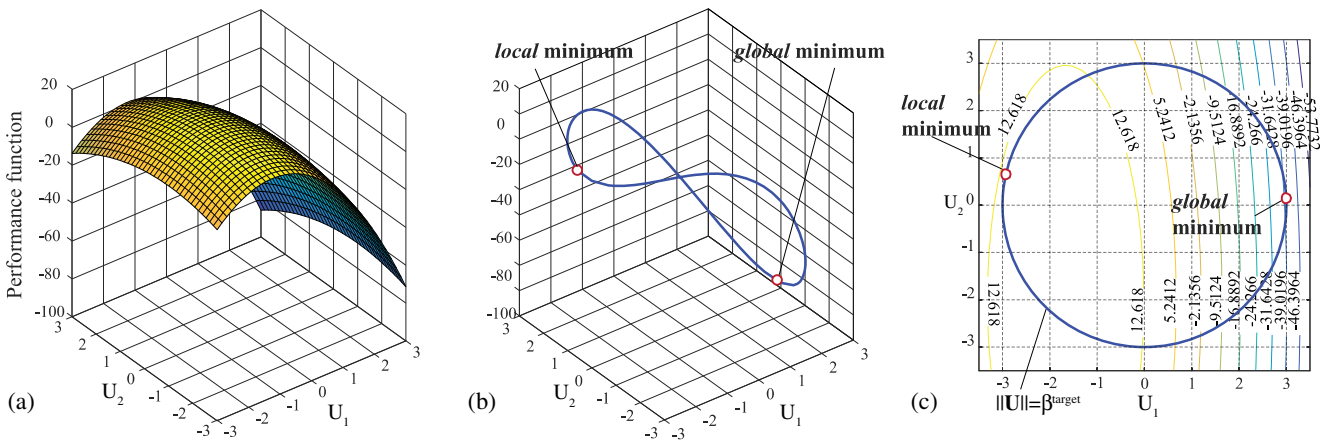

Fig. 2 **a** Performance function ($(\mu_{m1},\mu_{m2}) = (50,20), (\sigma_1,\sigma_2) = (30,10)$) plot in the standard normal space, **b** a feasible solution line for the lower level optimization problem, and **c** local and global minima on a contour plot of the performance function

Table 1 Two-bar truss optimization results and failure probabilities

	Optimization results			Failure probability		
U_0	Volume	Area 1	Area 2	FORM	SORM	MCS
(0.0,0.0)	17.64	2.52	3.36	1.35×10^{-3}	1.40×10^{-3}	1.38×10^{-3}
(−1.732,−1.732)	1.44	0.36	0.12	8.297×10^{-1}	8.411×10^{-1}	8.43×10^{-1}

$$\begin{aligned} \min_{\mathbf{d},\mu_{\mathbf{X}}} \quad & f(\mathbf{d},\mu_{\mathbf{X}}) \\ \text{s.t.} \quad & g_{P_f^{\text{target}}} \geq 0 \\ & \mathbf{d}^{\text{lower}} \leq \mathbf{d} \leq \mathbf{d}^{\text{upper}} \\ \text{with } & \mathbf{K}(\mathbf{d},\mathbf{X})\mathbf{u}(\mathbf{d},\mathbf{X}) = \mathbf{f}(\mathbf{X}) \end{aligned} \tag{8}$$

where $g_{P_f^{\text{target}}}$ is the performance function that is the P_f^{target} -quantile of the limit-state function g, alternatively obtained by

$$g_{P_f^{\text{target}}} = \arg\min_{G} \left\{ G(\mathbf{d},\mathbf{U}) \mid \|\mathbf{U}\| = \beta^{\text{target}} \right\} \tag{9}$$

In general, the PMA shows more efficient and robust convergence compared to the RIA (Tu et al. 1999). The PMA minimizes a complex objective function in (9) while satisfying a simple constraint function, whereas the RIA solves a minimization problem of a simple objective function with a complicated constraint function in (4).

2.2 Single-loop algorithm for RBTO

Efficiency in RBDO/RBTO can be improved by replacing the inner loop of the reliability analysis by a non-iterative procedure, which is often called single-loop scheme (Liang et al. 2004; Shan and Wang 2008). By enforcing the Karush-Kuhn-Tucker (KKT) optimality conditions of the probabilistic constraint in the reliability analysis, the constraint is replaced with an approximate deterministic constraint. In this approach, the optimal point in (9) should satisfy the following KKT optimality conditions:

$$\begin{aligned} \nabla_{\mathbf{U}} G(\mathbf{d},\mathbf{U}) + \lambda \cdot \nabla_{\mathbf{U}} \left(\|\mathbf{U}\| - \beta^{\text{target}} \right) = \mathbf{0} \quad & \text{(stationarity)} \\ \lambda \cdot \left(\|\mathbf{U}\| - \beta^{\text{target}} \right) = 0 \quad & \text{(complementary slackness)} \\ \|\mathbf{U}\| - \beta^{\text{target}} = 0 \quad & \text{(primal feasibility)} \end{aligned} \tag{10}$$

From the geometric interpretation (Liang et al. 2004), the solution $\mathbf{U}$ of (10) is derived as:

$$\mathbf{U} \equiv \mathbf{U}^{\text{t}} = \beta^{\text{target}} \left(-\frac{\nabla_{\mathbf{X}} g(\mathbf{d},\mathbf{X}(\mathbf{U}))\mathbf{J}_{\mathbf{X},\mathbf{U}}}{\|\nabla_{\mathbf{X}} g(\mathbf{d},\mathbf{X}(\mathbf{U}))\mathbf{J}_{\mathbf{X},\mathbf{U}}\|} \right) \tag{11}$$

where $\mathbf{J}_{\mathbf{X},\mathbf{U}}$ is the Jacobian of the transformation, $\mathbf{X}$ to $\mathbf{U}$ (see Der Kiureghian (2005) for more information about general transformation of random variables). Thus, the equivalent deterministic optimization problem is formulated as

$$\begin{aligned} \min_{\mathbf{d},\mu_{\mathbf{X}}} \quad & f(\mathbf{d},\mu_{\mathbf{X}}) \\ \text{s.t.} \quad & g(\mathbf{d},\mathbf{X}(\mathbf{U}^{\text{t}})) \geq 0 \\ & \mathbf{d}^{\text{lower}} \leq \mathbf{d} \leq \mathbf{d}^{\text{upper}} \\ \text{with } & \mathbf{K}(\mathbf{d},\mathbf{X}(\mathbf{U}^{\text{t}}))\mathbf{u}(\mathbf{d},\mathbf{X}(\mathbf{U}^{\text{t}})) = \mathbf{f}(\mathbf{X}(\mathbf{U}^{\text{t}})) \end{aligned} \tag{12}$$

Nguyen (2010) proposed a single-loop RBDO algorithm for *system* reliability analysis using the matrix-based system reliability (MSR) method (Song and Kang 2009). Numerical examples showed that the proposed single-loop system reliability-based design optimization (SRBDO) approach is efficient and accurate. This paper primarily focuses on single-loop (component) reliability topology optimization. Therefore, readers interested in system level constraints in optimization can refer to Nguyen (2010); and Nguyen et al. (2011).

2.3 Non-convexity of probabilistic constraints and the local optimum effects on RBTO results

A probabilistic constraint in RIA and PMA of RBTO requires using an optimization algorithm to find the MPP as a lower level optimization problem. Due to the characteristics of probabilistic constraints such as probability distribution functions, and transformation between physical space and normalized space used for reliability analysis, the lower level optimization problem is often non-convex in nature also referred as an NP-hard problem. The MPP is likely to be a local optimum and may cause the optimization to result in different results. The single-loop approach adopted in the paper utilizes the KKT *necessary* conditions to approximate the MPP from the performance function at each iteration of the optimization. A point satisfying the KKT conditions cannot guarantee global optimality unless the performance function is convex. For robustness-based design optimization, Guo et al. (2009a, 2009b, 2011) presented a method to perform confidence structural response analysis of truss structures considering ellipsoid static load uncertainty. The authors discussed convexity of functions in a robust optimization problem and proposed a method of a confidence single-level formulation for ellipsoidal load uncertainty by using Semidefinite Programming (SDP). That allows the reformulated lower level problem to be solved with global optimality. The global optimality of the probabilistic function is also a crucial consideration in RBTO; however,

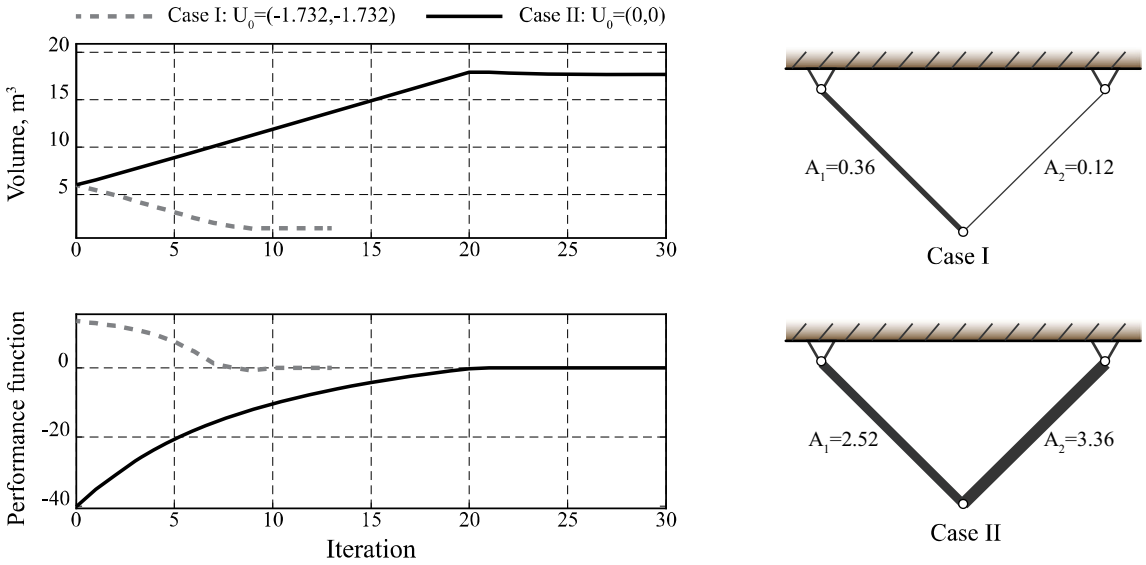

Fig. 3 Convergence histories and optimized bar sizes for case I and II

literary discussion is not as robust. In this section, we study the optimum state of a probabilistic compliance constraint transformed in PMA and its potential effects on converged results.

Now consider the two-bar truss structure illustrated in Fig. 1. The structure is subjected to a random horizontal force H with a mean μ_{m1} of 50 and a normal distribution having a standard deviation of σ_1=30; and a random vertical force V with a mean μ_{m2} of 20 and a normal distribution having a standard deviation of σ_1=10. The general form of the sizing optimization problem is as follows.

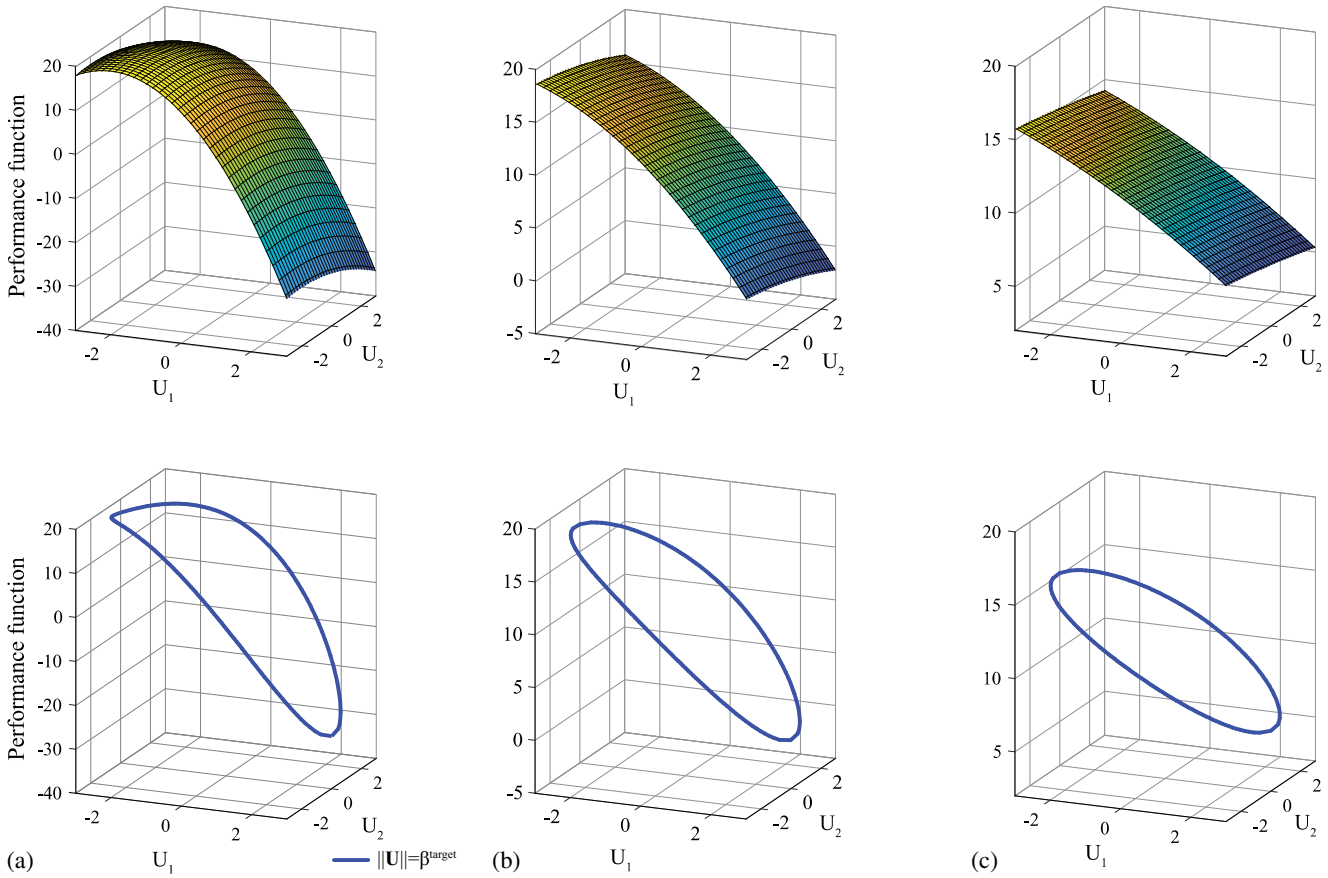

Fig. 4 Performance function ((μ_{m1},μ_{m2},) = (50,20)) plots for varying standard deviations. **a** (σ_1,σ_2) = (25,10), **b** (σ_1,σ_2) = (10,4), **c** (σ_1,σ_2) = (5,2)

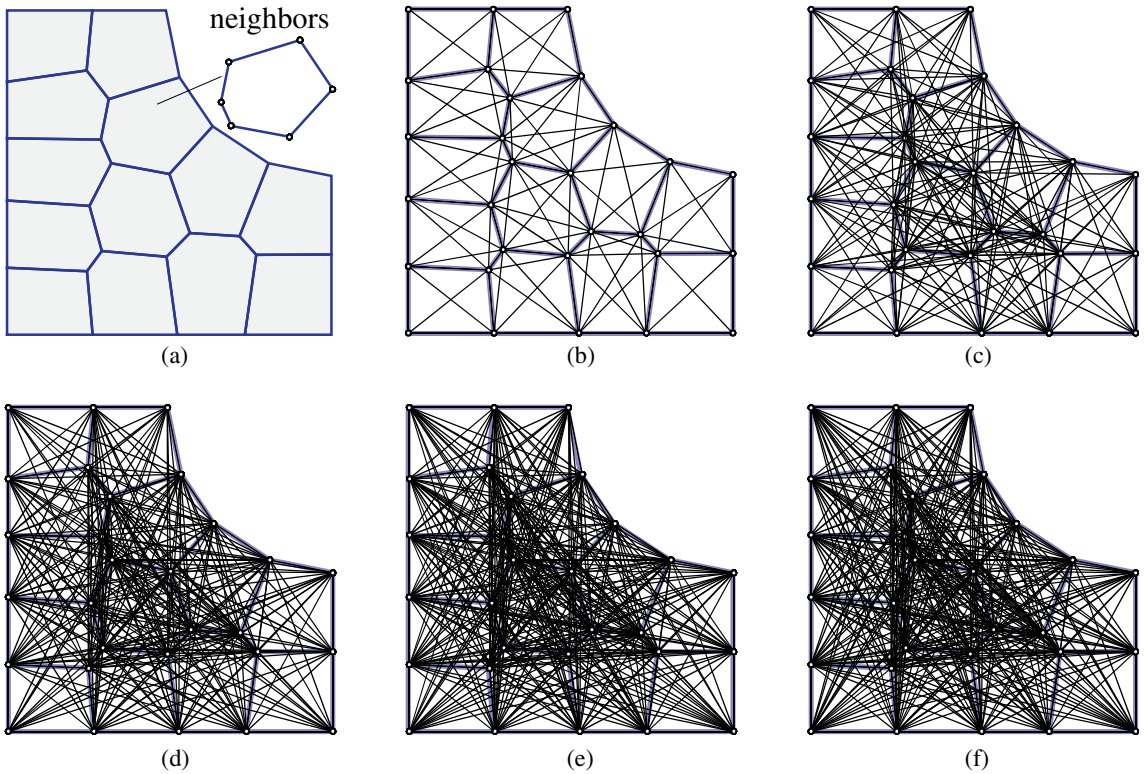

Fig. 5 Example of ground structure connectivity level generation. **a** Base mesh, **b** level 1 connectivity, **c** level 2 connectivity, **d** level 3 connectivity, **e** level 4 connectivity, and **f** full level connectivity

$$\begin{aligned} &\min_{\mathbf{A}} Vol = \sum_{i=1}^{2} A_i L_i \\ &\text{s.t. } P[g(\mathrm{H},\mathrm{V},\mathbf{A}) : 20 - c(\mathrm{H},\mathrm{V},\mathbf{A}) \le 0] \le P_f^{\text{target}} = 0.0013 \end{aligned} \tag{13}$$

where

$$\begin{aligned} &c(\mathrm{H},\mathrm{V},\mathbf{A}) = \sum_{i=1}^{2} \frac{f_i(\mathrm{H},\mathrm{V})^2 L_i}{E_i A_i} \\ &f_1(\mathrm{H},\mathrm{V}) = \frac{\mathrm{V}}{2\cos\alpha} - \frac{\mathrm{H}}{2\sin\alpha},\ f_2(\mathrm{H},\mathrm{V}) = \frac{\mathrm{V}}{2\cos\alpha} + \frac{\mathrm{H}}{2\sin\alpha} \end{aligned} \tag{14}$$

where Vol, A_i and L_i represent the truss volume, the cross-sectional area, and the length of member i, respectively. Moreover, c represents the compliance, and f_i denotes the force in member i, and E_i is Young's modulus of member i. In the PMA, the performance function is

$$\begin{aligned} &\min_{\mathbf{A}} G(\mathbf{U},\mathbf{A}) = 20 - \sum_{i=1}^{2} \frac{(\mathrm{U}_i\sigma_i + \mu_{mi})^2 L_i}{E_i A_i} \\ &\text{s.t. } \|\mathbf{U}\| = \beta^{\text{target}} = 3.0 \end{aligned} \tag{15}$$

Figure 2 shows the overall behavior of the performance function in the standard normal space U. In PMA-based RBTO, an optimal solution of a lower level problem in (13) should be located on a feasible solution line as shown in Fig. 2b, c. Given random variables and deterministic properties, global and local minimums can be identified at the first iteration of the double-loop optimization process. The performance function at the local minimum $\mathbf{U}^*_{\text{local}} = (-2.9173, 0.6997)$ that is found by solving a lower level optimization problem with initial guess $\mathbf{U}_{\text{initial}} = (-1.732, -1.732)$ is $g_{P^{\text{target}}}\left(\mathbf{U}^*_{\text{local}}\right) = 13.591$. Thus, the local minimum satisfies the inequality in (9). The performance function at the global minimum $\mathbf{U}^*_{\text{global}} = (2.9961, 0.1538)$ is $g_{P^{\text{target}}}\left(\mathbf{U}^*_{\text{global}}\right) = -40.092$. Note that the performance function shows the most negative value with respect to the compliance constraint at the global optimum and the local minimum is an infeasible point for the upper level optimization. Assume that a lower level optimization problem is numerically solved by an optimization algorithm with an initial guess that is an optimal point obtained from the previous iteration in (9). Reliability-based design optimization of the given problem considering two different initial guesses (Case I: $\mathbf{U}_0 = (-1.732, -1.732)$; Case II: $\mathbf{U}_0 = (0.0, 0.0)$) results in totally different bar sizes (see Table 1). The difference in bar sizes is mainly due to the inequality constraint of the optimization problem being satisfied in the local minimum condition and then in each iteration, $\mathbf{U}^*$ is trapped in the valley of the PMA function at the upper left of Fig. 2b.

The convergence histories of the objective function and the performance function are illustrated in Fig. 3. Although the optimization algorithm finds converged solutions satisfying the inequality constraint for both cases, the target failure of probability

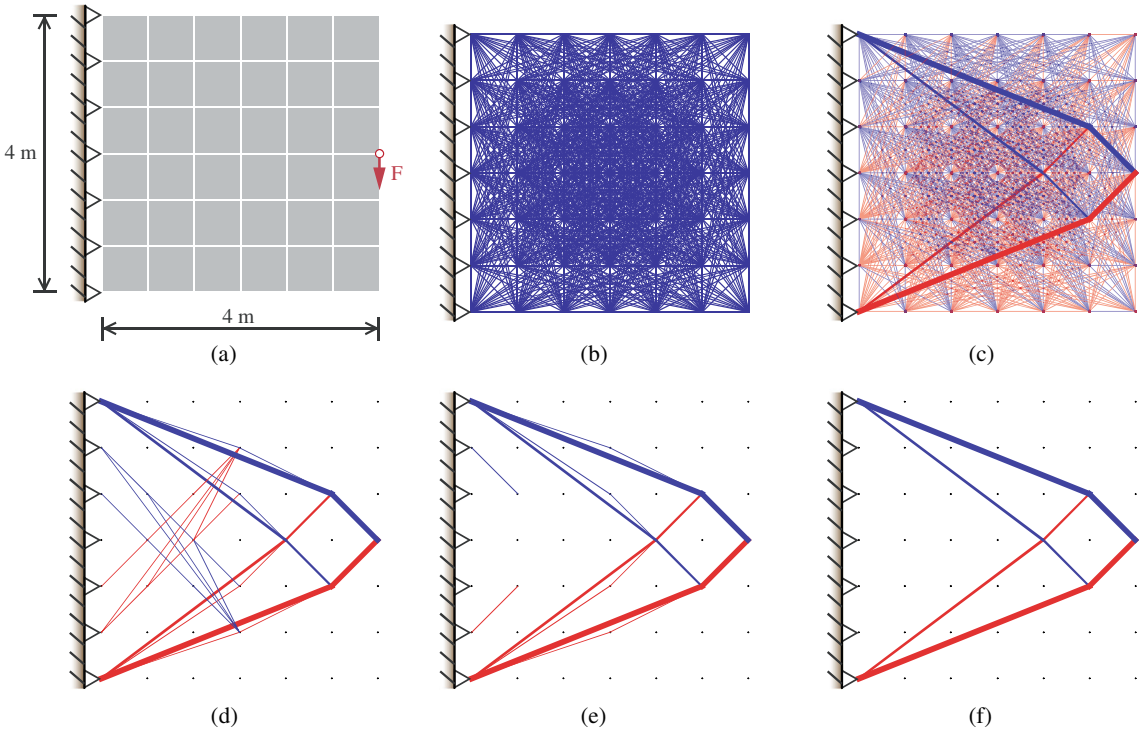

Fig. 6 Ground structure and filtered structure for DTO employing the conventional filtering approach: **a** design domain, loading and boundary conditions, **b** ground structure, **c** filtered structure ($\varepsilon_{\text{cut-off}}$=0.00), **d** filtered structure ($\varepsilon_{\text{cut-off}}$=0.0001), **e** filtered structure ($\varepsilon_{\text{cut-off}}$=0.001), and **f** filtered structure ($\varepsilon_{\text{cut-off}}$=0.1)

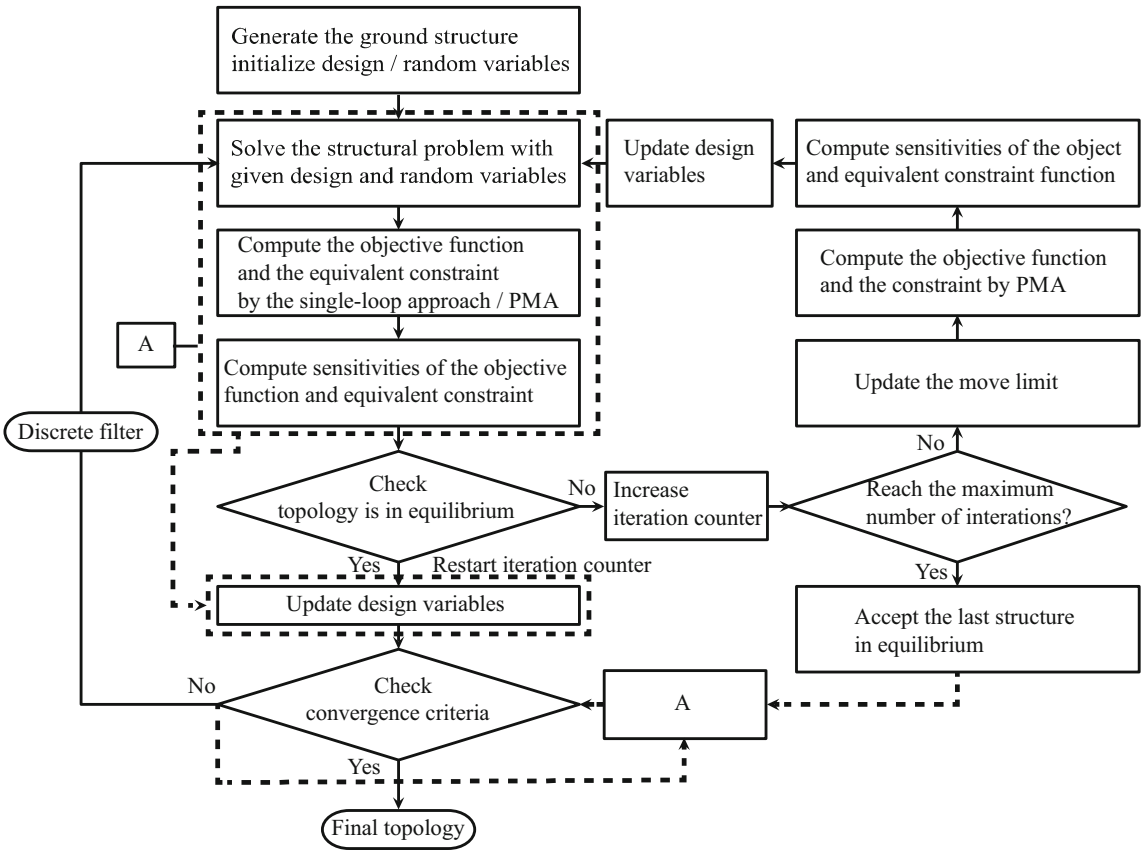

Fig. 7 Flowchart of the proposed optimization algorithm

for Case I is indeed violated. The failure probabilities for both results, computed by First-Second Order Reliability Method (FORM/SORM; Der Kiureghian 2005) and Monte Carlo Simulation (1×10^6 simulations) are shown in Table 1.

In contrast to the DTO case (Christensen and Klarbring 2009), when the compliance is mathematically expressed in the probabilistic form, it commonly becomes a concave function based on probabilistic distribution functions and transformation of its random variables to the standard normal space for reliability analysis using FORM and SORM. It is noted that the degree of concavity of probabilistic compliance function depends on types of random variables and standard deviation, correlation, etc. For instance, Fig. 4 illustrates performance functions of the given problem in the U space corresponding to different standard deviations of normally distributed and uncorrelated random variables. The overall concavity of the function decrease when a standard deviation of a random variable is relatively smaller than its mean value (e.g., small coefficient of variation) so that it reduces the existence of multiple local minima. Although finding global optimality with confidence is beyond the scope of this paper, it should be noted that RBDO/RBTO may suffer on finding feasible solutions due to the local minima as discussed above.

The single-loop approach adopted in this paper uses the KKT condition to approximately find a MPP in the lower level optimization problem. Since the performance function in the PMA-based RBTO is generally not a convex function, the solution from the KKT necessary conditions is not guaranteed as a global optimum. Therefore, the possibility of obtaining a local minimum from the approximated MPP by the single-loop approach still exists. In numerical applications of this paper, relatively small standard deviations of random variables are considered, and failure probabilities of optimized structures are computed and verified.

3 Discrete filtering

The set of interconnected bars is referred to as the ground structure in topology optimization of discrete structures. The size of the ground structure is dependent on the connectivity level that determines the interconnectedness of bars. To generate the ground structure, a design domain is discretized with elements, also known as a base mesh, shown in Fig. 5a. In the

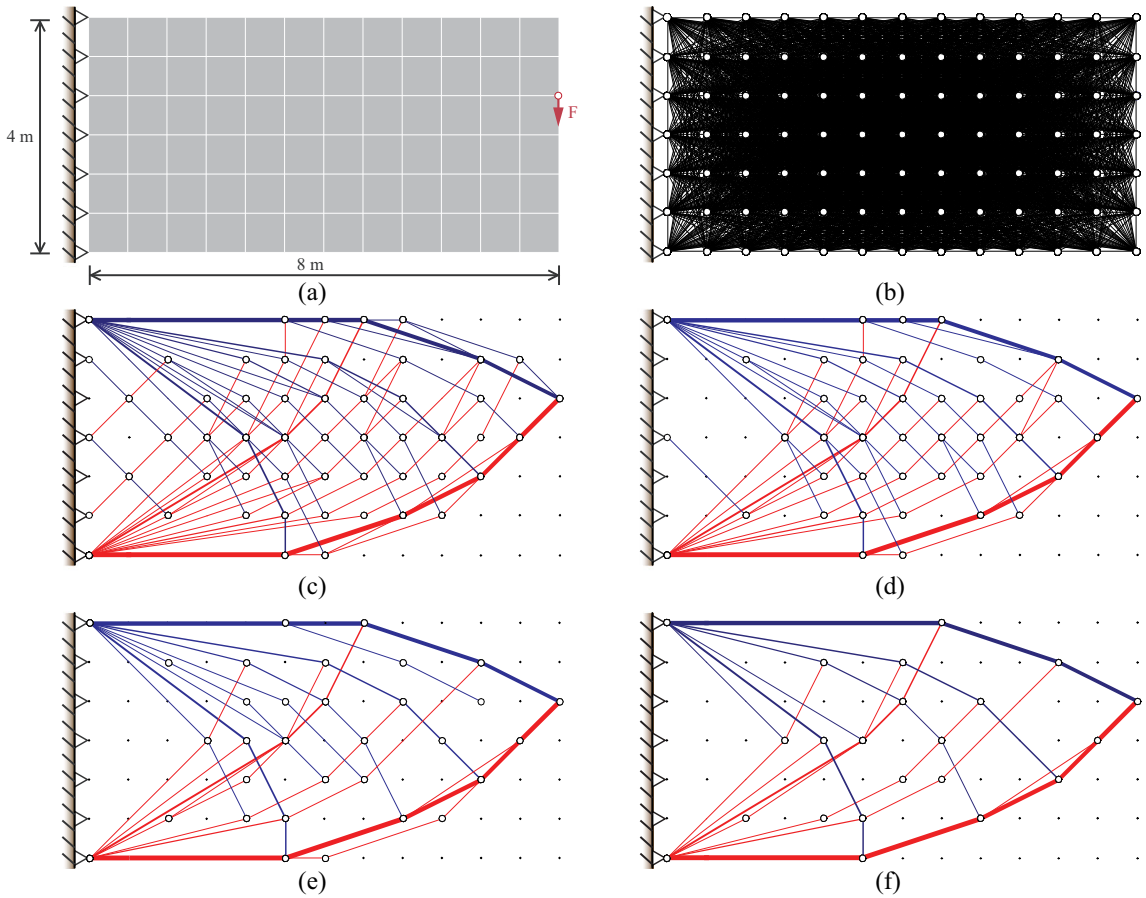

Fig. 8 Ground structure and filtered structures with varying $\varepsilon_{\text{cut-off}}$ for RBTO using the conventional filtering approach: **a** design domain, loading and boundary conditions, **b** full connectivity ground structure, **c** $\varepsilon_{\text{cut-off}} = 0.0001$, **d** $\varepsilon_{\text{cut-off}} = 0.005$, **e** $\varepsilon_{\text{cut-off}} = 0.02$, and **f** $\varepsilon_{\text{cut-off}} = 0.05$

base mesh, two nodes are considered *neighbors* if they belong to the same element, and the connectivity level defines subsequent surrounding nodes to which each node can be connected. For instance, a node will only be connected to its neighbors in connectivity level 1 as shown in Fig. 5b. Level 2 connectivity will generate bars up to the immediate surrounding nodes of its neighbors (Fig. 5c). Similarly, level 3 connectivity will generate bars up to the subsequent neighboring nodes surrounding level 2 (Fig. 5d). 'A full connectivity level' refers to a ground structure where all nodes are interconnected within a design domain.

In the context of deterministic topology optimization (DTO), a compliance minimization problem with a volume constraint is formulated as

$$\begin{aligned} &\min_{\mathbf{A}} \quad \mathbf{f}^{\mathrm{T}}\mathbf{u}(\mathbf{A}) \\ &\text{s.t.} \quad \sum_{i=1}^{ne} A_i L_i \le V_c \\ &\qquad \mathbf{A}^{\text{lower}} \le \mathbf{A} \le \mathbf{A}^{\text{upper}} \\ &\text{with } \mathbf{K}(\mathbf{A})\mathbf{u}(\mathbf{A}) = \mathbf{f} \end{aligned} \tag{16}$$

where L_i is the length of truss element i, ne is the number of truss elements, and $\mathbf{A}$ is the vector of cross-sectional areas. A lower bound on each design variable is commonly assigned to avoid a singular stiffness matrix during topology optimization. Conventional topology optimization of truss structures using the ground structure approach implements a filtering process with a cut-off value $\varepsilon_{\text{cut-off}}$ after the optimization processes are complete. That is, truss elements smaller than the cut-off value are eliminated, and the filtered truss structure is subsequently considered as the final topology. This end-filtering process is used to interpret the final structure from the ground structure.

DTO with the conventional filtering method is illustrated through a cantilever beam optimization problem. The rectangular cantilever beam in Fig. 6a is clamped on the left side and loaded by a vertical force F at mid-height of the right side. Using the ground structure approach, the structural domain is discretized into a finite spatial distribution of nodes that are each connected to every other node with truss members as shown in Fig. 6b. Figure 6c through f shows final topologies after optimization according to varying cut-off values (increasing from 0 to 0.1). It should be noted that the determination of a proper cut-off value is ambiguous and is often based on a process of trial and error. For example, a small cut-off value may lead to many thin elements, which cannot be practically built, while a larger cut-off value may result in a rigid-body motion (mechanism) or hanging member shown in Fig. 6e. In addition, the end-filtering process may change the final compliance and cause the problem of violating global equilibrium.

To address these issues, Ramos Jr. and Paulino (2016) recently proposed a discrete filtering scheme that enables filtering of well-defined (e.g., satisfying the global equilibrium) structures from ground structures. The discrete filtering process is performed with updated design variables at each optimization iteration according to:

$$\text{Filter}(\mathbf{A}, \alpha_f) = \begin{cases} 0 & \text{if } A_i/\max(\mathbf{A}) < \alpha_f \\ A_i & \text{otherwise} \end{cases}, \quad 0 \le \alpha_f \le 1 \tag{17}$$

It is noted that α_f was adopted in the range of 1% from a practical point of view in Ramos Jr. and Paulino (2016). After the discrete filtering, global equilibrium is checked to ensure that the filtered structure is well defined. If the global equilibrium is violated, the move limit in the Optimality Criteria (OC) for updating design variables is adjusted to a smaller value, and the discrete filtering technique is performed again. These steps are repeated until the global equilibrium is satisfied or the number of checking processes reaches the prescribed maximum iteration. However, some structures satisfying global equilibrium may be singular due to aligned hinges and/or detached degrees of freedom. To handle the singularity of the structural system, minimization of potential energy with Tikhonov regularization is adopted. Thus, it allows for a zero bound on the design variables. Using this approach, the regularized compliance minimization problem in DTO can be formulated as:

$$\begin{aligned} &\min_{A} \quad \mathbf{f}^{\mathrm{T}}\mathbf{u}(\mathbf{A}) \\ &\text{s.t.} \quad \sum_{i=1}^{ne} A_i L_i \le V_c \\ &\qquad \mathbf{0} \le \mathbf{A} \le \mathbf{A}^{\text{upper}} \text{with } \mathbf{A} = \text{Filter}(\mathbf{A}, \alpha_f) \\ &\text{and} \quad \min_{\mathbf{u}} \prod(\mathbf{u}(\mathbf{A})) + \frac{\lambda}{2}\mathbf{u}(\mathbf{A})^{\mathrm{T}}\mathbf{u}(\mathbf{A}) \end{aligned} \tag{18}$$

where λ denotes a small positive number, and Π(·) represents the potential energy of the system defined as:

Table 2 Influence of filtering method on actual probabilities of the optimal topology for the cantilever beam problem (target failure probability, $P_f^{\text{target}} = 0.005$)

Conventional filtering method				
$\varepsilon_{\text{cut-off}}$	0.05	0.02	0.005	0.0001
Volume	369.76	379.14	385.48	386.48
$\|\|\mathbf{Ku-f}\|\|/\|\|\mathbf{f}\|\|$	5.78×10^{-2}	1.32×10^{-2}	8.51×10^{-7}	3.99×10^{-7}
P_{FORM}	1.00	1.00	6.13×10^{-3}	5.01×10^{-3}
P_{MCS}	1.00	1.00	6.24×10^{-3}	5.08×10^{-3}
Discrete filtering method				
α_f	0.05	0.02	0.005	0.0001
Volume	407.39	395.68	386.91	387.93
$\|\|\mathbf{Ku-f}\|\|/\|\|\mathbf{f}\|\|$	4.42×10^{-7}	4.52×10^{-7}	4.62×10^{-7}	3.65×10^{-7}
P_{FORM}	5.00×10^{-3}	5.00×10^{-3}	5.00×10^{-3}	5.00×10^{-3}
P_{MCS}	5.05×10^{-3}	5.05×10^{-3}	5.06×10^{-3}	5.05×10^{-3}

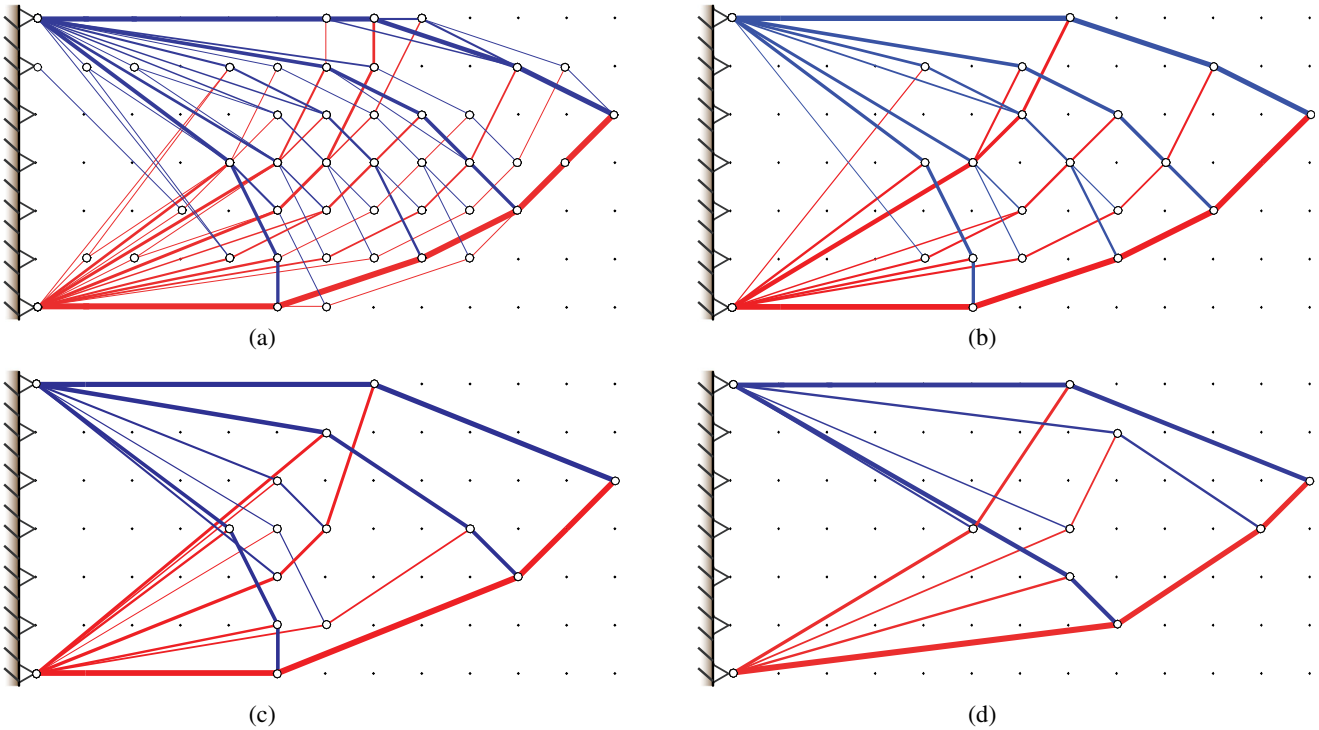

Fig. 9 Filtered structures by RBTO with varying discrete filter values: **a** $\alpha_f = 0.0001$, **b** $\alpha_f = 0.005$, **c** $\alpha_f = 0.02$, and **d** $\alpha_f = 0.05$

$$\prod(\mathbf{u}(\mathbf{A})) = \frac{1}{2}\mathbf{u}(\mathbf{A})^{\mathrm{T}}\mathbf{K}(\mathbf{A})\mathbf{u}(\mathbf{A}) - \mathbf{f}^{\mathrm{T}}\mathbf{u}(\mathbf{A}) \tag{19}$$

The particular solution of displacements of the linear system is obtained by minimizing the potential energy with Tikhonov regularization as follows:

$$(\mathbf{K}(\mathbf{A}) + \lambda\mathbf{I})\mathbf{u}(\mathbf{A}) = \mathbf{f} \tag{20}$$

The structure is considered to be in global equilibrium if the following inequality holds:

$$\|\mathbf{K}(\mathbf{A})\mathbf{u}(\mathbf{A}) - \mathbf{f}\| \le \gamma\|\mathbf{f}\| \tag{21}$$

where γ is a prescribed tolerance (e.g., $\gamma = 10^{-4}$).

By incorporating the discrete filtering scheme into the RBTO framework, one can obtain an optimal

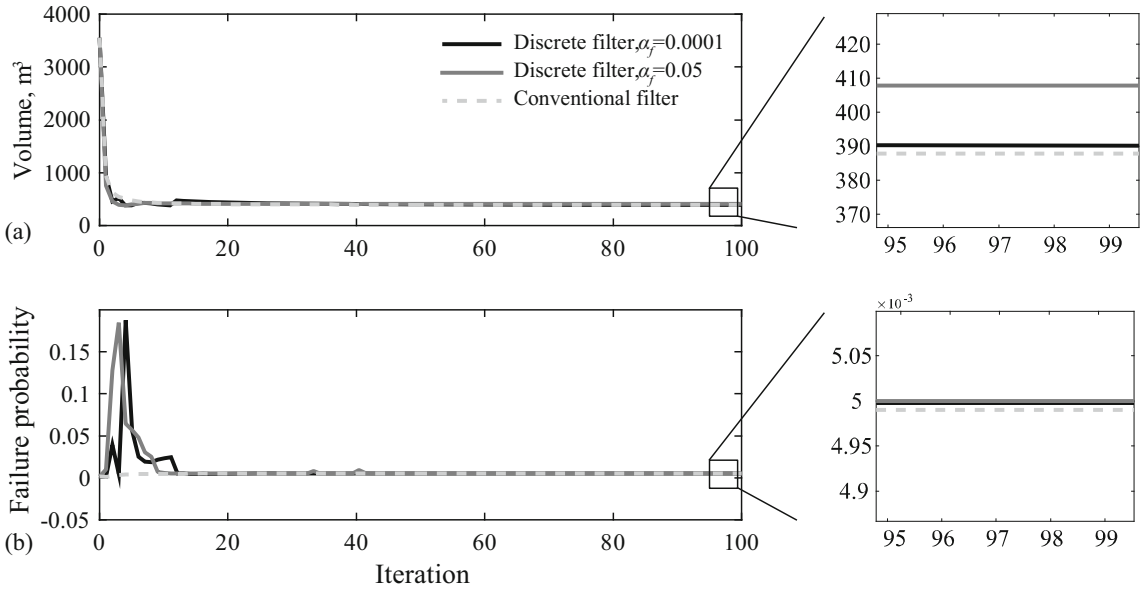

Fig. 10 Convergence histories of the cantilever problem: **a** volume, and **b** failure probability

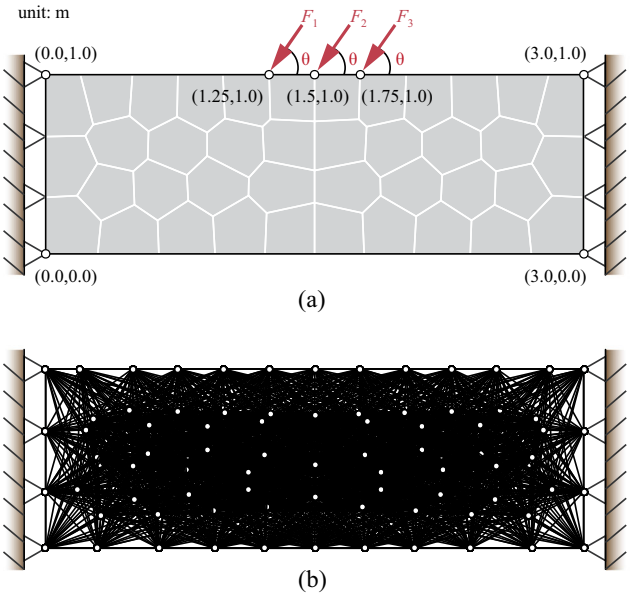

Fig. 11 Clamped beam problem: **a** loadings and boundary conditions, and **b** level 4 connectivity ground structure

topology of a structure under uncertainties using a ground structure model as follows:

$$\begin{aligned} &\min_{\mathbf{A},\boldsymbol{\mu}_\mathbf{X}} \quad f(\mathbf{A},\boldsymbol{\mu}_\mathbf{X}) \\ &\text{s.t.} \quad g(\mathbf{A},\mathbf{X}(\mathbf{U}^{\mathrm{t}}))\geq 0 \\ &\qquad \mathbf{0}\leq\mathbf{A}\leq\mathbf{A}^{\mathrm{upper}} \\ &\text{with} \quad \mathbf{A}=\mathrm{Filter}(\mathbf{A},\alpha_f) \\ &\text{and} \quad \min_{\mathbf{u}} \quad \prod(\mathbf{A}(\mathbf{d},\mathbf{X}(\mathbf{U}^{\mathrm{t}}))) + \frac{\lambda}{2}\mathbf{u}(\mathbf{A},\mathbf{X}(\mathbf{U}^{\mathrm{t}}))^{\mathrm{T}}\mathbf{u}(\mathbf{A},\mathbf{X}(\mathbf{U}^{\mathrm{t}})) \end{aligned} \tag{22}$$

The proposed optimization algorithm is illustrated by a flowchart as shown in Fig. 7. This paper implements Ramos Jr. and Paulino (2016) method into single-loop RBTO so that it can solve the singularity of the structural system after the discrete filter is carried out, and identify the structure in global equilibrium, while satisfying the target failure probability.

As a ground structure undergoes many iterations to reach optimal design, many of design variables, such as highly redundant bars are imposed zero areas using the discrete filter. Thus, computational times of general structural analysis and reliability analysis in RBTO can be reduced by excluding zero areas for stiffness matrix assembly, structural analysis, sensitivity calculations as well as reliability analysis. In contrast, RBTO using the conventional filtering approach maintains the same number of design variables because removal of bars, i.e. assigning zero areas to bars which have less cross-sectional area than the cut-off filter value, is performed after optimization is completed. Further reduction of the overall computational cost can be considered as a synergistic aspect of combining single-loop RBTO with a discrete filter.

4 Comparative study and numerical applications

The proposed RBTO using the ground structure method with the discrete filtering approach is demonstrated by numerical examples where the design variables are cross-sectional areas, and the objective function is the total volume. The probabilistic constraint is defined in terms of the compliance with the upper limit $C_{\max}$ such as $P(\mathrm{g(X)} = C_{\max} - \mathrm{C} \leq 0) \leq \mathrm{P}_f^{\mathrm{target}}$. Applied forces, force direction, and Young's modulus are considered as random variables following normal distributions. However, it should be noted that the application of the proposed method is not limited to normal distributions. Different combinations of random variables and statistical dependency are considered in RBTO, which will be stated for each numerical example. Although only the compliance constraint is considered in this paper, different types of design criteria such as stress (Ohsaki 2010; Hemp 1973), buckling failure and nodal instability (Tyas et al. 2006; Guo et al. 2005; Descamps and Filomeno Coelho 2014; Mitjana et al. 2018), and natural frequency (Jin and De-yu 2006) have been studied for multidisciplinary design and applications. As a structure endures various demands on its capacity, combinations of design consideration for objective and constraint functions are of great interest for practical design and applications. In the probabilistic design approach, the failure event associated with combinations is often formulated as a system event such as a logical or Boolean function of multiple failure modes. The system event is evaluated by system reliability analysis and incorporated in the system reliability-based design optimization. The readers can refer to (Royset et al. 2001; Ba-abbad et al. 2006; Nguyen 2010) for more details on the system reliability-based design optimization.

The optimality criteria (OC) (Bendsøe and Sigmund 2003; Groenwold and Etman 2008; Ramos Jr. and Paulino 2016) is utilized as the update scheme. For the first two numerical problems, the FORM and the Monte Carlo Simulation

Table 3 Parameter values of random variables used for the clamped beam problem

E (N/m^2)		$F1$ (N)		$F2$ (N)		$F3$ (N)		θ (N)	
$\mu_{\mathrm{m}E}$	$\sigma_{\mathrm{s}E}$	$\mu_{\mathrm{m}F1}$	$\sigma_{\mathrm{s}F1}$	$\mu_{\mathrm{m}F2}$	$\sigma_{\mathrm{s}F2}$	$\mu_{\mathrm{m}F3}$	$\sigma_{\mathrm{s}F3}$	$\mu_{\mathrm{m}\theta}$	$\sigma_{\mathrm{s}\theta}$
100,000	7,500	600	150	900	90	700	140	45	6.82

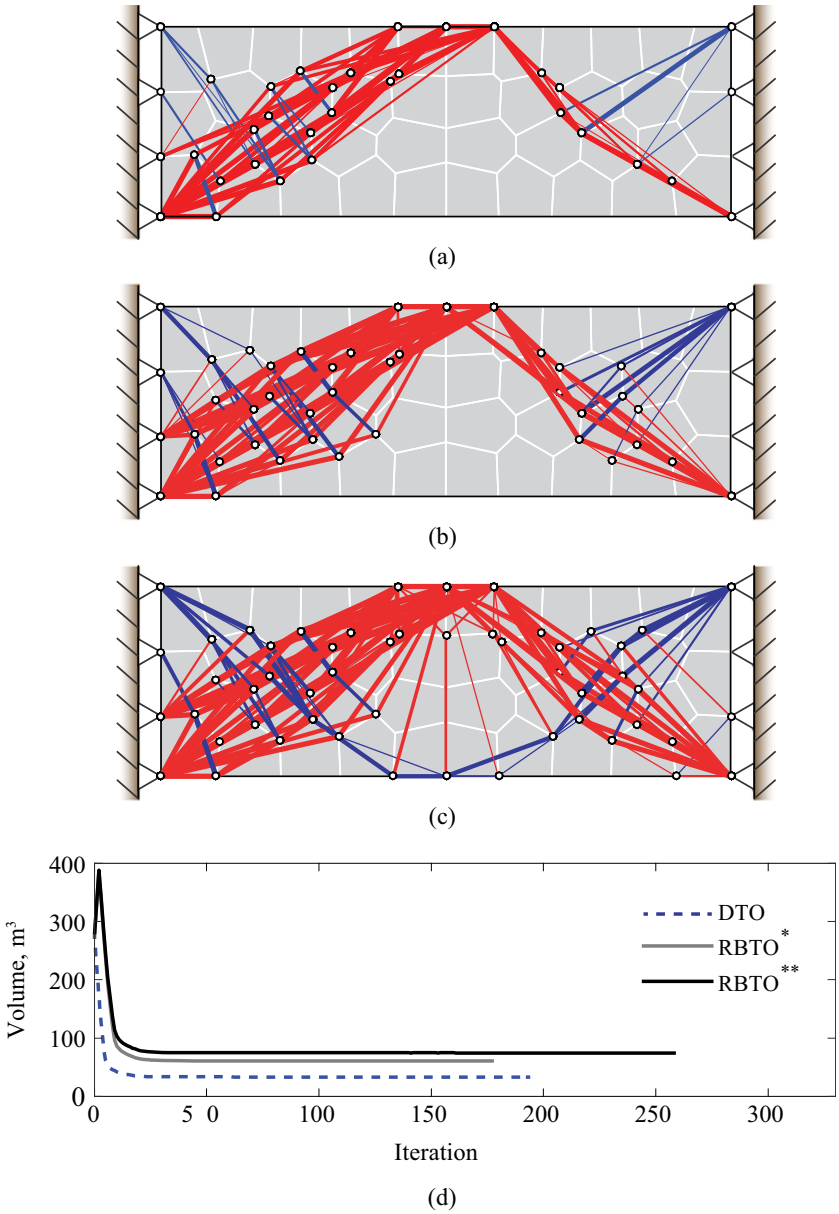

Fig. 12 Topology optimization results by discrete filter ($\alpha_f = 0.01$): **a** DTO (volume = 33.35 m^3, $P_{MCS} = 6.56 \times 10^{-1}$), **b** RBTO*—Case I (volume = 60.82 m^3, $P_{FORM} = 5.00 \times 10^{-3}$), **c** RBTO**—Case II (volume = 74.67 m^3, $P_{FORM} = 5.00 \times 10^{-3}$), and **d** convergence histories

(MCS) are also performed to check whether the optimal structure filtered by the conventional method and the proposed method satisfies the target failure probability. It should be noted that minimization of potential energy with Tikhonov regularization is used to solve the singular system in the FORM and the MCS.

4.1 Comparison between conventional filtering approach and discrete filtering approach in RBTO

First, the conventional and discrete filters are imposed on a cantilever beam optimal design to demonstrate the effects of varying filter input parameters $\varepsilon_{\text{cut-off}}$ and α_f on

Table 4 Summary of comparison between RBTO and DTO for varying safety factors

Safety factor	1.25	1.5	1.75	2.0	2.121	2.25	2.5
P_{f_FORM}	0.2256	0.0872	0.0293	0.0088	0.0050	0.0029	0.0009
Volume (DTO), m^3	43.50	54.06	65.32	78.05	84.71	91.97	106.78
P_f^{target}	0.2256	0.0872	0.0293	0.0088	0.0050	0.0029	0.0009
Volume (RBTO), m^3	42.78	51.68	60.82	70.27	74.66	78.76	87.90
Difference, %	1.67	4.61	7.41	11.07	13.46	16.77	21.48

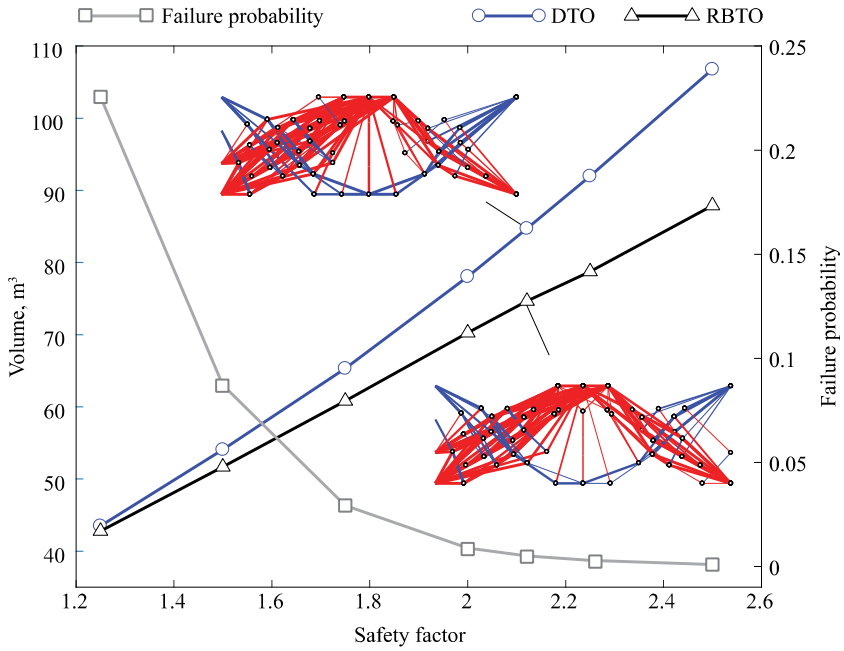

Fig. 13 Optimal structure volume (left y axis) and graphic representation of volume difference from DTO and RBTO. Calculated failure probability (right y axis) at corresponding a safety factor (x-axis) using connectivity level four for a ground structure

the final topologies. The cantilever design domain clamped on the left and loaded on the right by a vertical force at two thirds-height is discretized with 12×6 elements (Fig. 8a). A full connectivity level ground

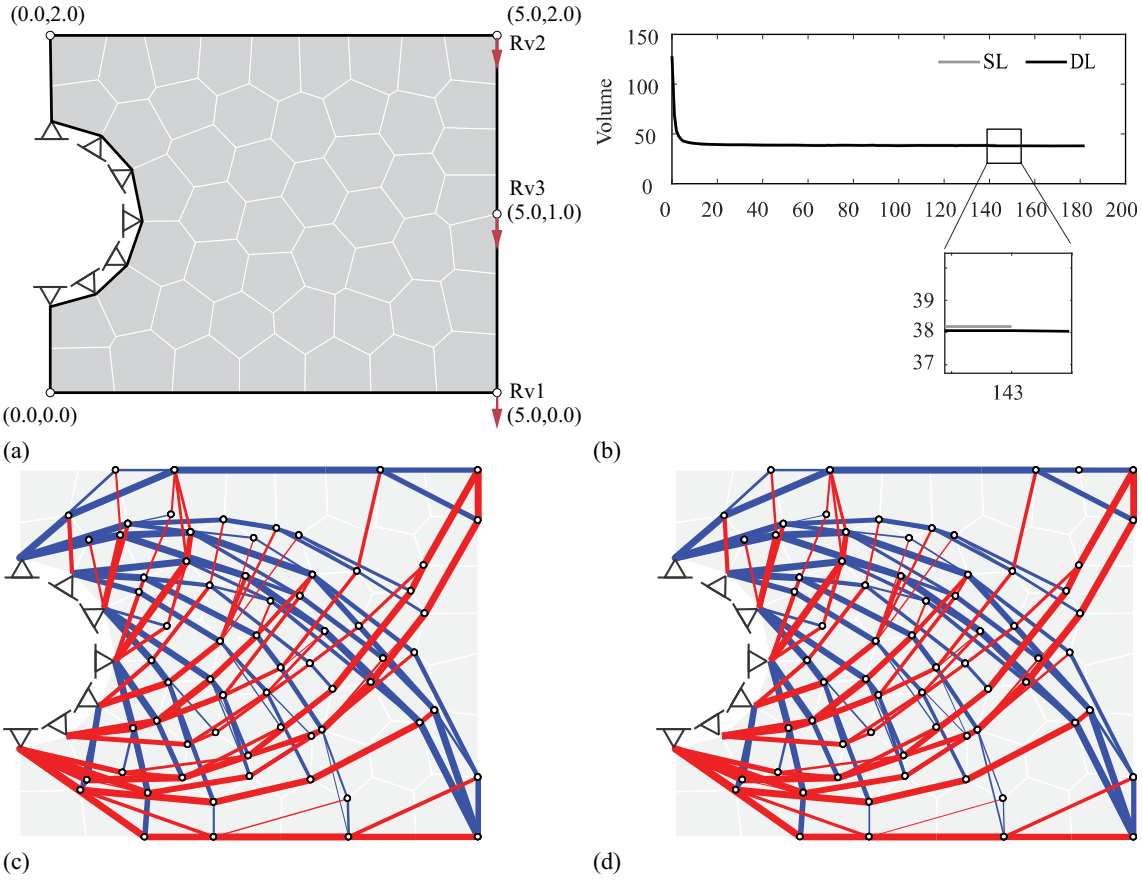

Fig. 14 **a** Applied forces Rv1, Rv2, Rv3 on given design domain with boundary condition, **b** convergence history plot using single-loop (SL) and double-loop (DL) algorithms in RBTO, **c** optimal topology using SL RBTO, and **d** optimal topology using DL RBTO. Note that the results of an optimization problem considering the level 2 connectivity and two random variables, Rv1 and Rv2 are presented

Table 5 The number of bars and parameter values for random variables used in comparative study of SL RBTO and DL RBTO

Connectivity level	1	2	3	4
Number of bars	504	1,284	2,199	3,106
Random variable	Rv1	Rv2	Rv3	
Mean	120	150	120	
Standard deviation	12	15	12	

structure is generated as shown in Fig. 8b. To incorporate uncertainties in material properties and the load, Young's modulus E and the force F are modeled as random variables following the normal distributions with means ($\mu_{mE} = 10{,}000$ N/m^2, $\mu_{mF} = 100$ N) and standard deviations ($\sigma_{sE} = 750$ N/m^2, $\sigma_{sF} = 20$ N), respectively. The objective function is the total volume, and the probabilistic constraint is defined as $P\ (g(\mathrm{X}) = 5 - C \leq 0) \leq 0.005$. The initial cross-sectional areas are set to 0.5 m^2. The optimization results from Eq. (12) according to varying cut-off values $\varepsilon_{\text{cut-off}}$ of the conventional filter are illustrated in Fig. 8c through f. In addition, using a certain cut-off value can lead to a final topology including hanging members, which are not connected to the structure. A filter value with $\varepsilon_{\text{cut-off}} = 0.05$ eliminates relatively larger sizes of bars from a converged ground structure. Such bars removed by the conventional filter can greatly decrease stiffness and increase structural compliance. As a result, the filtered structure is highly likely to be an infeasible design and violate the probabilistic compliance constraint. The influence of the cut-off values on actual failure probabilities of the optimal topology is checked by use of the FORM and the MCS (Table 2). As the selected $\varepsilon_{\text{cut-off}}$ increases for the filtering process, a failure probability higher than the target probability is observed. That is, the conventional filtering approach may lead to the violation of the prescribed target failure probability.

Next, the same optimization problem is solved using the proposed method while varying discrete filtering values α_f. A discrete filter is activated with each iteration of optimization. Often, bars to be eliminated by the discrete filter have very low sensitivities of a probabilistic constraint with respect to design variables. The discrete filter prevents dramatic changes in structural responses of a filtered structure at each iteration. In addition, a gradient-based optimization algorithm can effectively search for optimum design based on the sensitivity of the probabilistic constraint while ensuring global equilibrium. These characteristics of a converged solution allow for a feasible design in global equilibrium with a certain level of reliability. Figure 9 shows filtered structures, which are in global equilibrium. In all plots, tension members are shown in blue and compression members in red. The thicknesses of the lines indicate the normalized area of truss elements to the maximum member area. Unlike the conventional approach, the proposed method is able to find feasible solutions that satisfy the target failure probability as confirmed in Table 2. Figure 10 shows the convergence history of the volumes and failure probabilities of the conventional and discrete filtering approaches in RBTO for 100 iterations. The non-smooth zig-zag pattern observed in the convergence plot within the first fifty

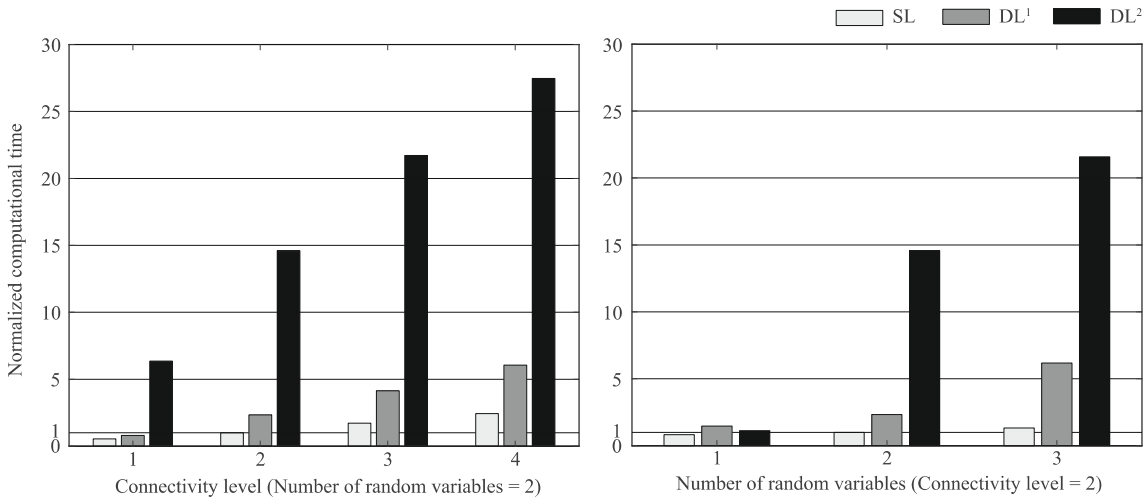

Fig. 15 Normalized computational times for SL and DL RBTO regarding (**a**) connectivity levels, and (**b**) number of random variables. Computational times are normalized with respect to the single-loop computation (12.5 s in this case) with connectivity level 2 and two random variables. (SL single-loop algorithm, DL^1 double-loop algorithm with initial guess of $\mathbf{U}^*$ obtained in a previous step, and DL^2 double-loop algorithm with a fixed initial guess of $\|\mathbf{U}_0\| = \beta$ at every iteration

Table 6 Parameter values of the random variables used for the curved cantilever structure problem

E (N/m^2)		F_1 (N)		F_2 (N)		F_3 (N)		F_4 (N)	
μ_{mE}	σ_{sE}	μ_{mF1}	σ_{sF1}	μ_{mF2}	σ_{sF2}	μ_{mF3}	σ_{sF3}	μ_{mF4}	σ_{sF4}
100,000	7,500	50	10	80	12	45	6.75	35	5.25

iterations is primarily due to the discrete filtering, which actively eliminates bars with areas smaller than the prescribed filtering value α_f.

4.2 Comparison of DTO and RBTO

In this example of the clamped beam (Fig. 11), the results by DTO and RBTO are compared to investigate the influence of the uncertainties on the optimal topologies. Note that, for DTO, the random variables in RBTO are replaced by deterministic parameters whose values are the same as the mean values. Five statistically independent random variables are used to describe forces (F_1, F_2, F_3), force angle (θ) and material property represented by Young's Modulus (E). All random variables are assumed to follow normal distributions. Figure 11a shows the design domain fixed on both left and right sides. Three parallel forces with a random angle θ are applied at the center region of the top edge of the design domain. The design domain is discretized with 40 polygonal elements after 100 Lloyd's iterations (Talischi et al. 2012), as shown in Fig. 11a. On the other hand, the ground structure with a level 4 connectivity (1,858 design variables) is illustrated in Fig. 11b. Table 3 lists the mean value μ_m and standard deviation σ_s for each random variable. The target failure probability of the compliance limit-state function $P_f^{\text{target}} = 0.005$, the upper bound of design variable $A^{\text{upper}} = 1.0$ m^2, the discrete filter coefficient $\alpha_f = 0.01$, and $C_{\max} = 8$ are used in optimization.

To verify the effects of the random variable θ on the final topology, two cases are considered for RBTO: (Case I) four random variables of F_1, F_2, F_3, E and deterministic force angle θ, and (Case II) five random variables of F_1, F_2, F_3, E, and θ. Figure 12 shows the optimal configuration of bar connectivities and sizes from DTO and RBTO. Due to the risk caused by the uncertainties, increased bar areas and additional connectivities are observed in RBTO compared to those from DTO. In addition, dominant directions of bar connectivities are observed between the forces and supports as shown in Fig. 12a and b. Additional consideration of the random variable θ (Case II) results in the creation of arch-shape connectivities towards the center at the bottom in Fig. 12c, primarily due to the possibility of forces with $\theta > 45°$ that cause the further increase in compliance. Therefore, the compliance will be reduced by providing the arch-shape connectivities. The convergence history in Fig. 12d confirms that the proposed method is able to find the optimal solution efficiently. In engineering practice, deterministic design generally adopts safety coefficients such as a safety factor, load and resistance factors to account for inherent uncertainties and natural randomness. The failure probability of the deterministic result (Fig. 12a) under the five random variables used for RBTO is provided in the paper, however, this does not suggest an actual collapse or failure of the structure. Further study on DTO with safety factors and comparison to RBTO are described in the following section.

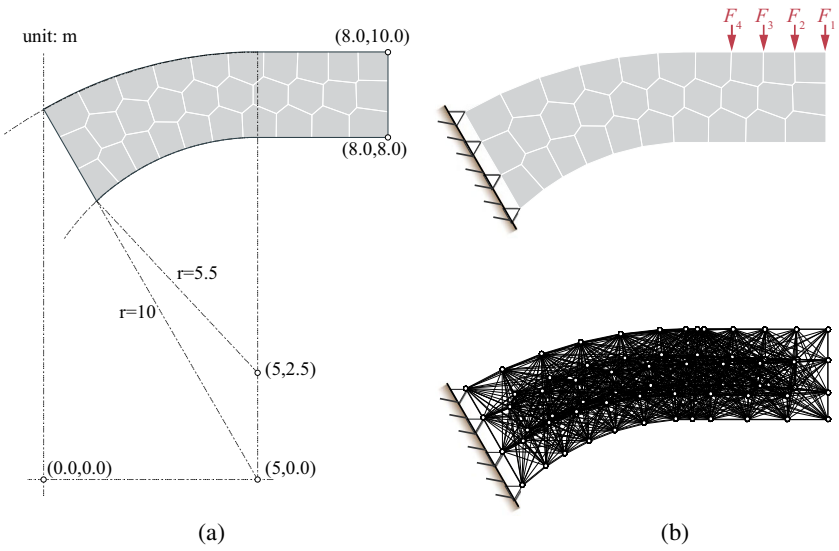

Fig. 16 Curved beam problem: **a** design domain, and **b** loadings and boundary conditions, and level 3 connectivity ground structure

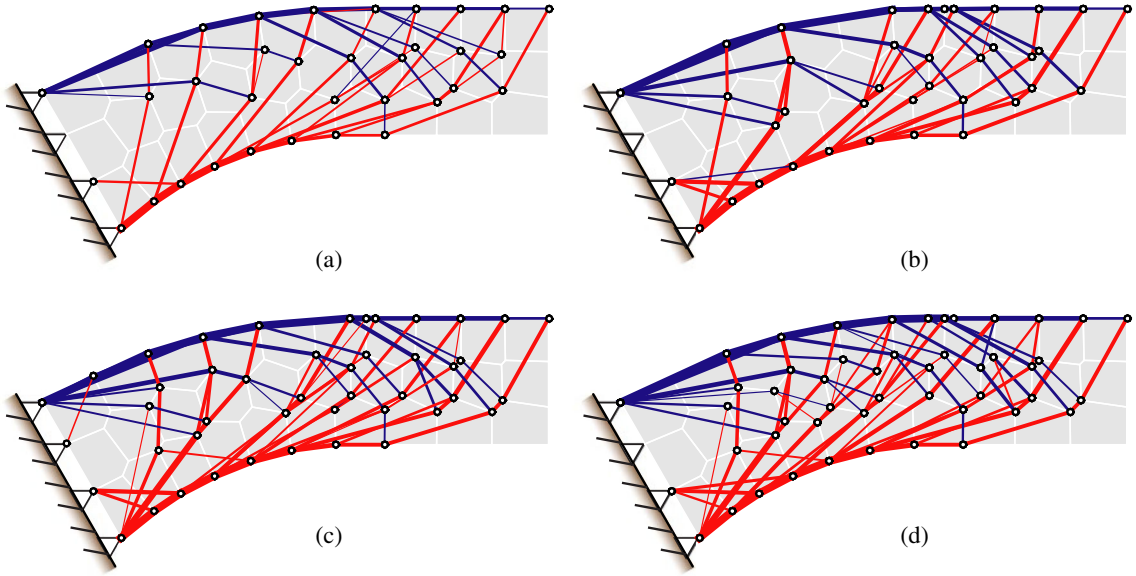

Fig. 17 Topology optimization results by a discrete filter ($\alpha_f = 0.01$): **a** DTO (volume = 54.73 m^3, $P_{\mathrm{MCS}} = 7.56 \times 10^{-1}$), **b** RBTO, $\rho_{ij} = 0.0$ (volume = 90.79 m^3, $P_{\mathrm{FORM}} = 7.50 \times 10^{-3}$), **c** RBTO, $\rho_{ij} = 0.5$ (volume = 105.39 m^3, $P_{\mathrm{FORM}} = 7.50 \times 10^{-3}$), and **d** RBTO, $\rho_{ij} = 0.75$ (volume = 113.91 m^3, $P_{\mathrm{FORM}} = 7.50 \times 10^{-3}$)

4.3 Comparison of RBTO and DTO considering varying safety factors

A numerical comparison between optimum designs of DTO and RBTO is presented with varying safety factors from 1.25 to 2.5. The same design domain, material properties, and random variables following a normal distribution, as described in Section 4.2, are used for the comparison study. The safety factor is defined as the ratio between the allowable compliance and the maximum compliance. When the optimal design is achieved in DTO, reliability analysis using the FORM is performed to compute the probability of failure of the structure. The probability of failure in DTO from the FORM analysis is imposed as a target failure probability in RBTO to compare the results from DTO, and RBTO approaches. The failure probability and volume of the optimal design in DTO corresponding to each safety factor are tabulated in Table 4. An optimal volume of a structure in RBTO with a target failure probability,

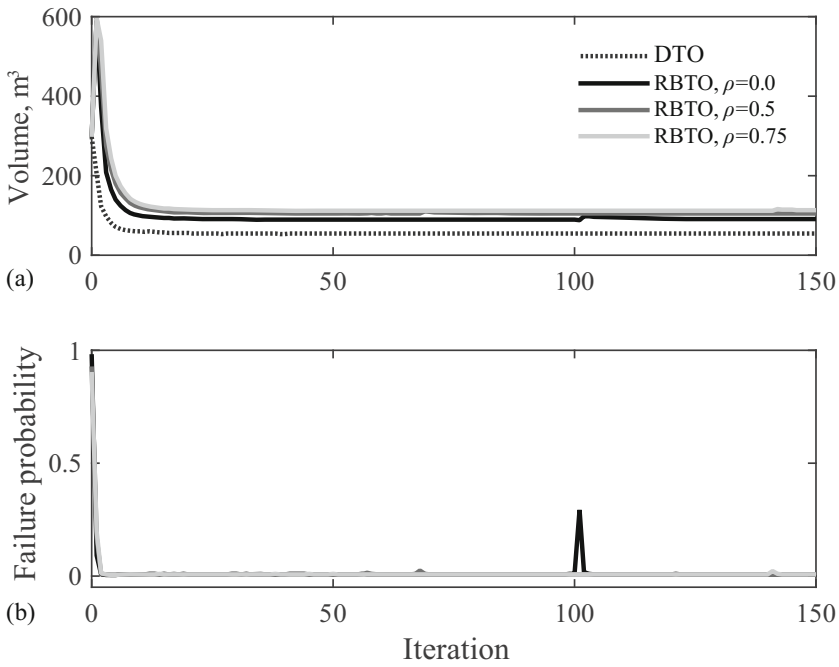

Fig. 18 Convergence histories of the curved beam problem: **a** volume, and **b** failure probability

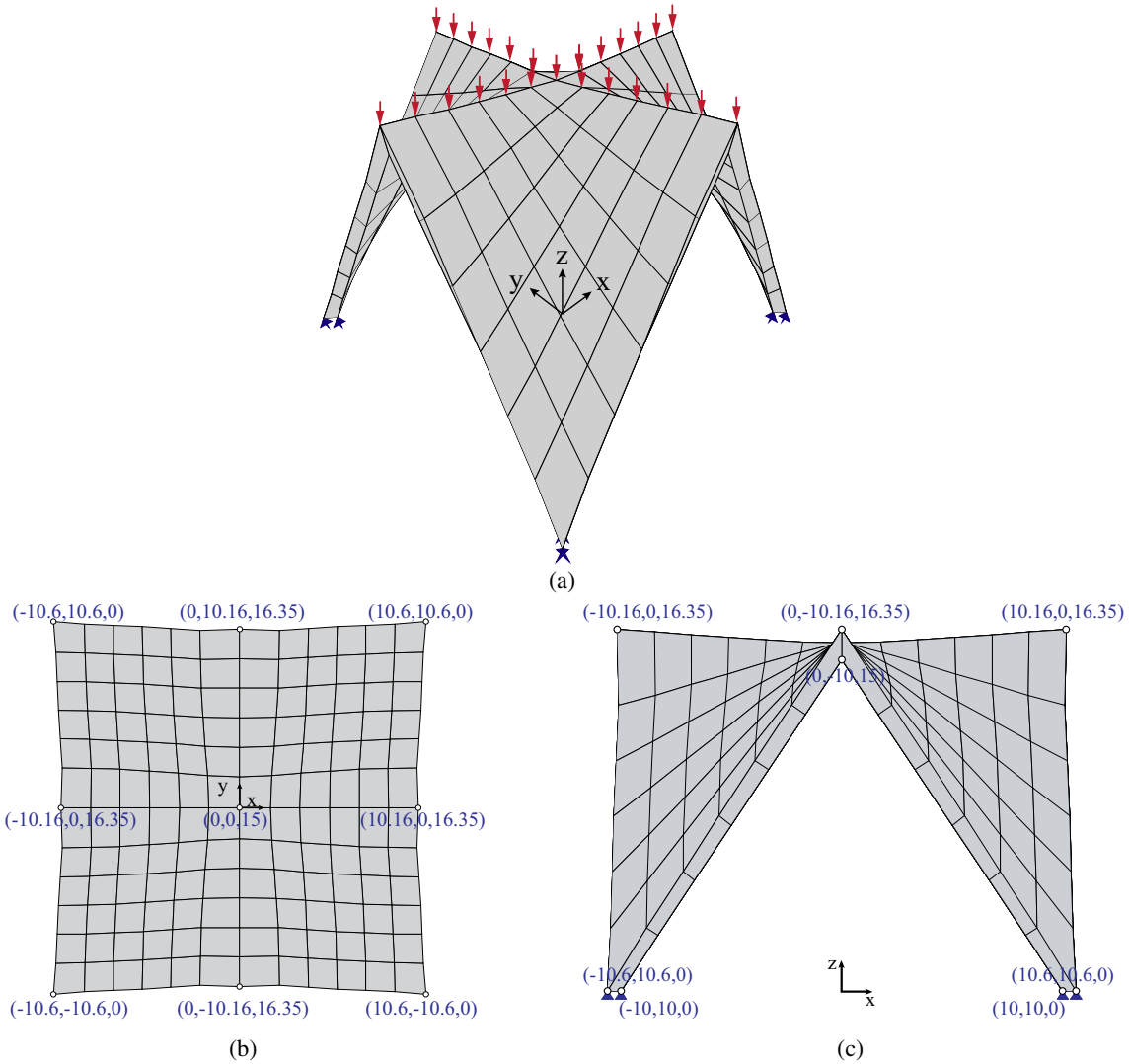

Fig. 19 Roof structure optimization example: **a** roof structure domain, loadings and boundary conditions, **b** top view, and **c** side view

and the failure probability in DTO, are summarized in Table 4. Figure 13 shows a higher optimal volume achieved by DTO when compared to an optimal structure from RBTO, while the probability of failure is the same for both structures. The optimal volume increases when a higher safety factor is imposed in DTO. When matching the safety factor with RBTO, DTO produces an optimized structure with a greater volume, suggesting a sub-optimal result. Given that converged solutions from RBTO and DTO are probably local minima due to possible non-convexity of the given problem, the RBTO design is closer to the global optimum design. As presented in Fig. 13, DTO and RBTO result in different optimal topologies of a structure under the equivalent probability of failure. Based on the present study, diverse solutions for a given optimization problem are expected to be found from RBTO, and DTO optimization approaches.

4.4 Comparison of computational time of single-loop RBTO and double-loop RBTO

Computational time for RBTO using single-loop (SL) algorithm in (12) and double-loop (DL) algorithm in (8) are compared in this section. Figure 14a shows the geometry and boundary conditions of a design domain used for the computational cost study. The optimization problem is comprised of one probabilistic constraint with respect to compliance. Random variables are forces, following the normal distribution, that are applied at the points shown in Fig. 14a. The different number of design variables and random variables in RBTO are used to show comprehensive differences with respect to computational cost. A ground structure of the design domain is constructed with four different connectivity levels to visualize the effects of the different number of design

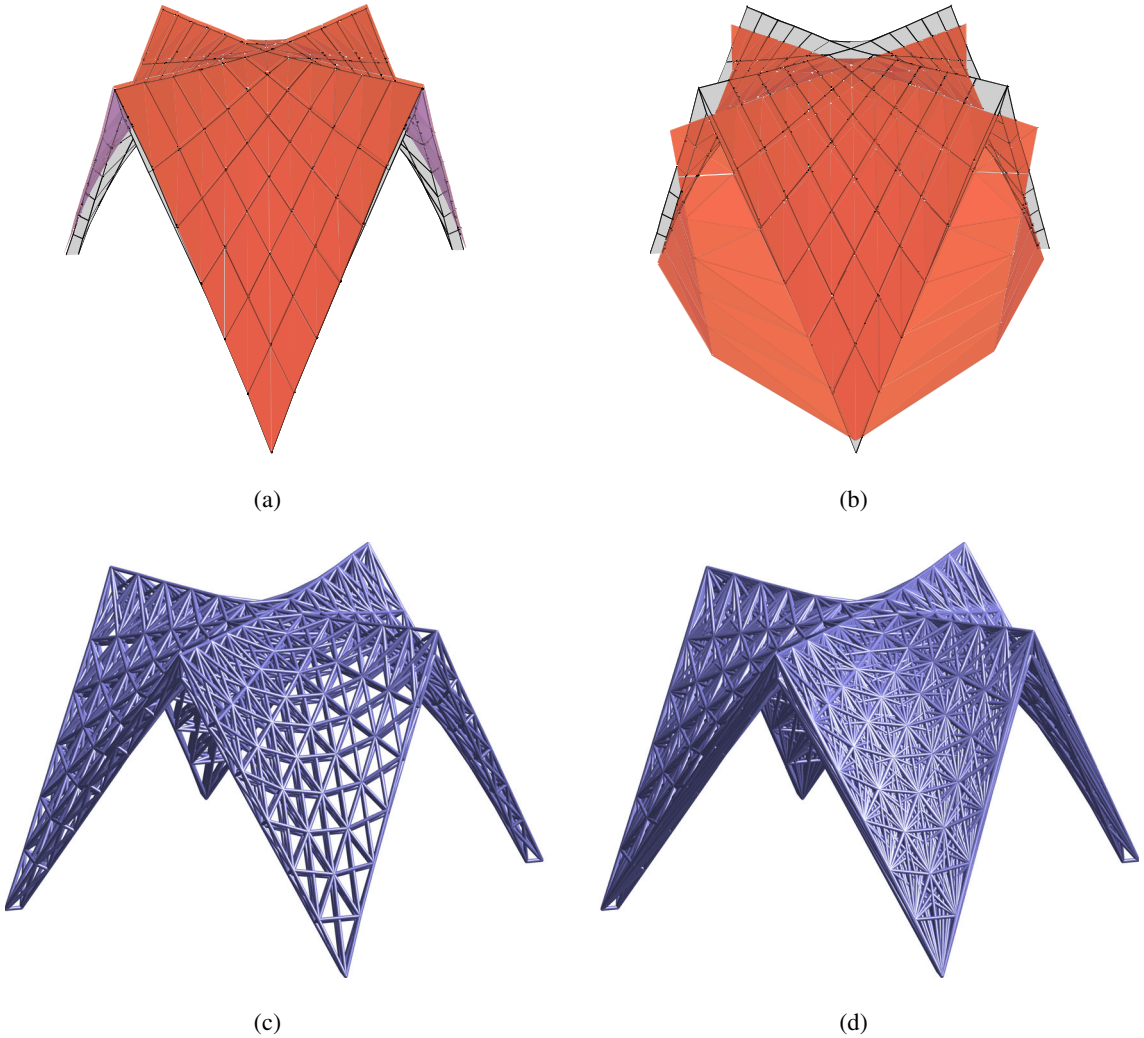

Fig. 20 Ground structure: **a** upper restriction surface, **b** lower restriction surface. **c** Level 1 connectivity (2,569 design variables), and **d** level 4 connectivity (7,995 design variables)

variables in RBTO on computational cost. The number of bars generated based on the connectivity level, the mean and standard deviation of random variables are summarized in Table 5.

The double-loop approach solves a lower level optimization problem to find MPPs (e.g., $||\mathbf{U}^*|| = \beta$) using reliability analysis. In this study, two different initial points are also considered in addition to the connectivity level for the lower level optimization procedure. The initial points, $\mathbf{U}_0$ satisfying $||\mathbf{U}_0|| = \beta$ at the first iteration, are selected, and new MPPs are found through optimization. Subsequent design variables are updated with sensitivity analysis of current design from the new MPPs. For each iteration in RBTO, MPPs obtained from the previous iterative step are used as starting points to identify new MPPs of the sub-optimization procedure in the updated design. Another consideration for $\mathbf{U}_0$ in sub-optimization is using the same fixed points $||\mathbf{U}_0|| = \beta$ for every iteration in RBTO. When level 2 connectivity and two random variables, Rv1 and Rv2 are considered in a optimization problem, optimal topologies from SL (Single Loop) RBTO and DL (Double Loop) RBTO and their convergence history are illustrated in Fig. 14b through d.

Table 7 Parameter values of the probabilistic constraint and random variables, and the discrete filter used for the roof structure problem

E (GPa)		F (kN)		$C_{\max}$	P_f^{target}	α_f	A^{upper} (m^2)
μ_{mE}	σ_{sE}	μ_{mF}	σ_{sF}	10	0.0025	0.01	1.5
200	40	100	20				

Figure 15 shows the average computational time for five analyses, of each different case, carried out to 70 optimization iterations. Times are normalized with respect to the SL RBTO method with level 2 connectivity considering two random variables. Figure 15, however, does not include the initialization time such as meshing design domain, or generating the ground structure. The computational cost of RBTO using the DL algorithm is heavily dependent on the selection of initial points for lower level optimization. Using DL RBTO with

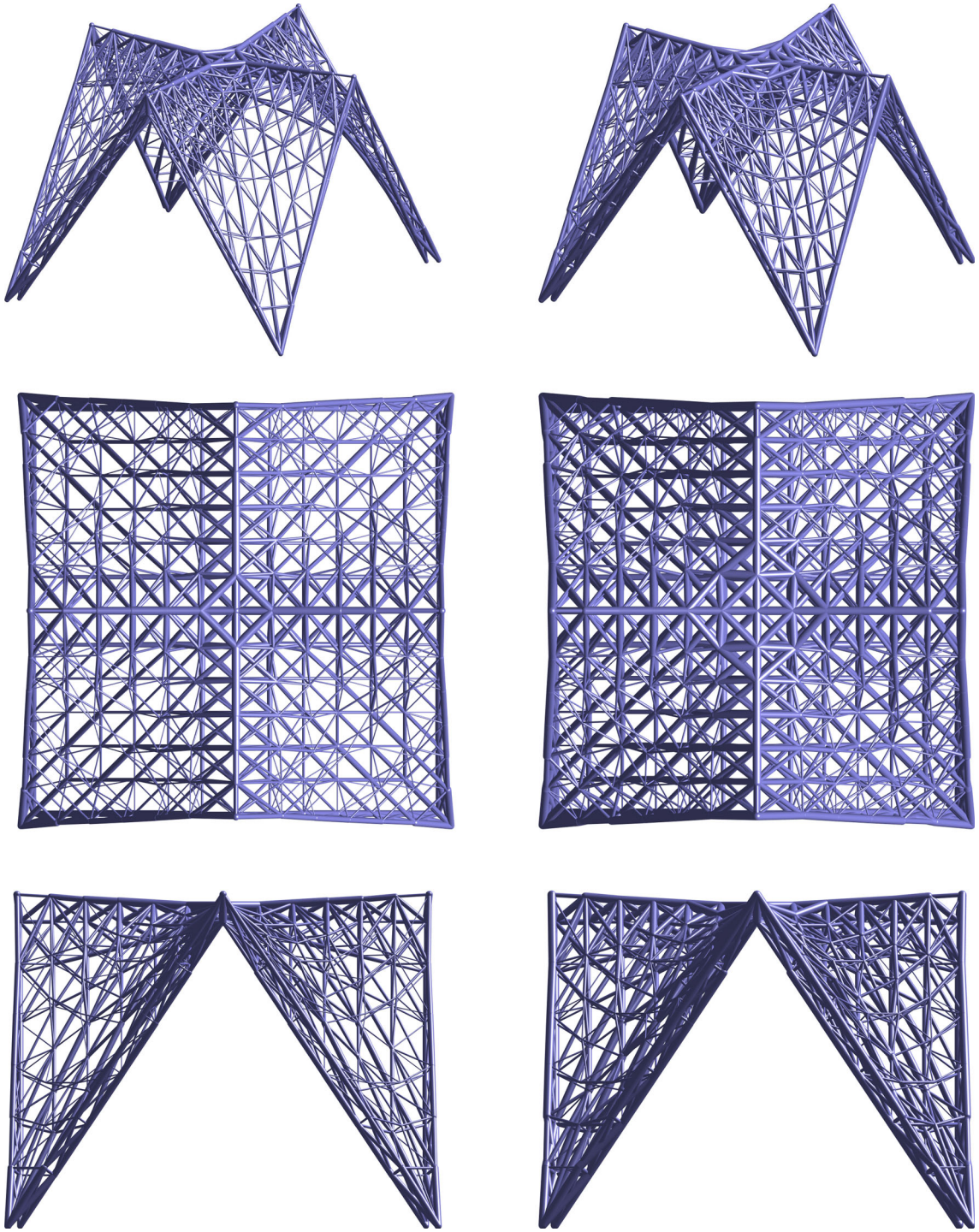

Fig. 21 Final topology by discrete filter ($\alpha_f = 0.01$, level 1 connectivity): **a** DTO, and **b** RBTO ($P_f^{\text{target}} = 0.0025$)

fixed $\mathbf{U}_0$ requires about eight times more computational cost than using the single-loop RBTO (level four connectivity and two random variable case in Fig. 15a). However, the increased computational time of DL RBTO is reduced when using $\mathbf{U}_0$ obtained from previous iterations.

Computational cost analysis with the varying random variables is presented in Fig. 15b, which shows the number of random variables does not significantly increase the overall computational cost. However, in SL RBTO, the outer loop, which includes structural and sensitivity analysis, updating

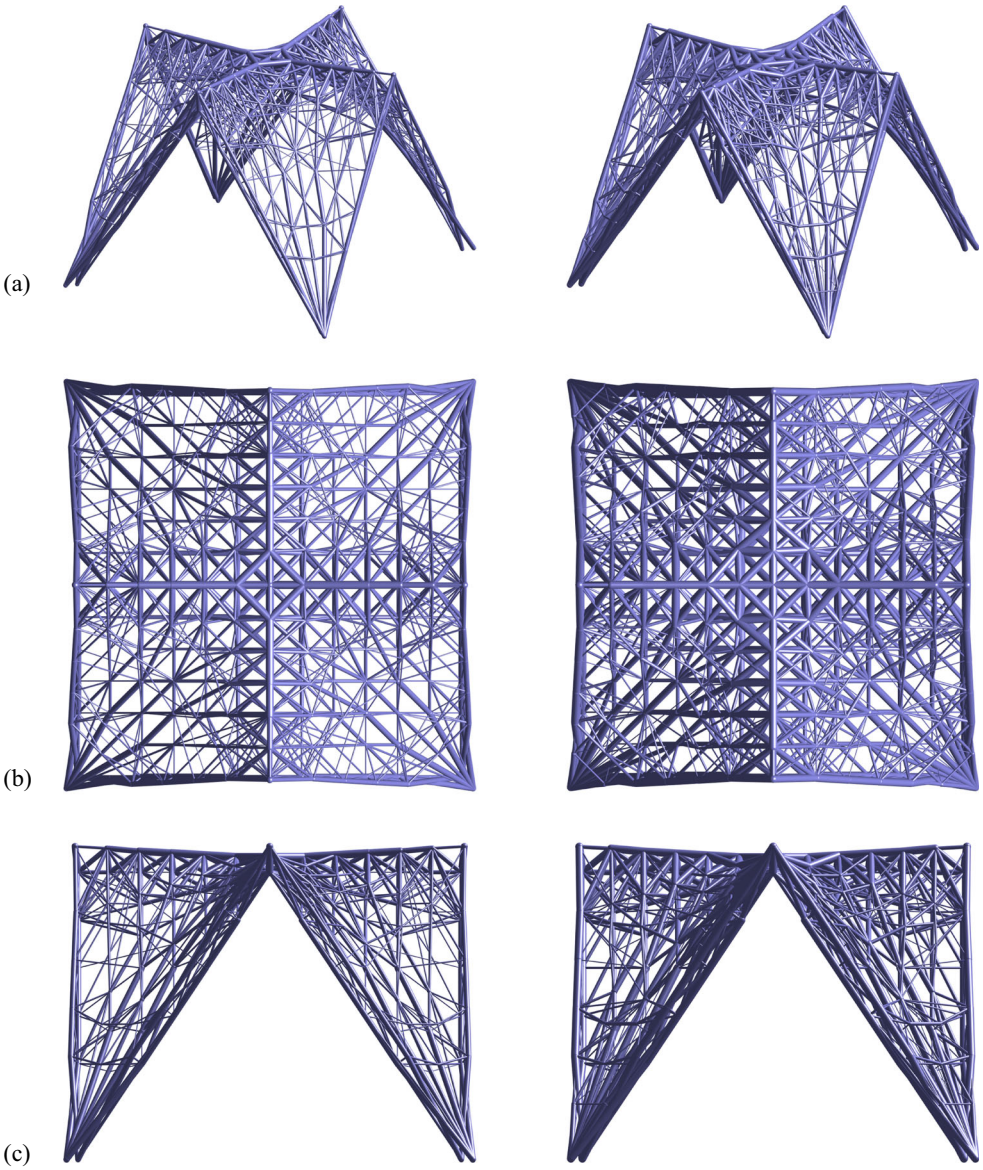

Fig. 22 Final topology by discrete filter ($\alpha_f = 0.01$, level 4 connectivity): **a** DTO, and **b** RBTO ($P_f^{\text{target}} = 0.0025$)

design variables significantly affects the overall computational cost. The increase in overall computation cost using the double-loop method with a higher number of random variables highlights the efficacy of the single-loop algorithm in RBTO. Considering average computation time represented in Fig. 15a, the number of random variables and problem sizes are significant factors affecting computational cost. Taken together, RBTO with the single-loop algorithm is a more computationally efficient optimization method when considering the different number of design and random variables (Table 5).

4.5 Curved cantilever structure optimization

Next, the proposed method is applied to design a curved cantilever truss clamped on the left side to demonstrate how the correlation affects the spatial distribution of structural members. The design domain discretized with 30 polygonal elements, after 100 Lloyd's iterations, is shown in Fig. 16a. The ground structure for a level 3 connectivity is then generated using "GRAND" (Zegard and Paulino 2014), which generates a ground structure with a total of 981 truss members. The limit-state function is defined on the compliance computed with multiple loads, i.e., $g(\mathbf{A},\mathbf{X}) = 8 - C(\mathbf{A},\mathbf{X})$. Young's Modulus E and forces F_i, $i = 1,\ldots, 4$, are assumed to be normal random variables. The mean and the standard deviation of each random variable are shown in Table 6. The target failure probability, the upper bound of design variables, and the discrete filter coefficient are set to $P_f^{\text{target}} = 0.0075$, $A^{\text{upper}} = 4.0\ \text{m}^2$, and $\alpha_f = 0.01$, respectively. The correlation coefficient $\rho_{ij},\ i \neq j,\ i,\ j = 1,\ldots, 4$, between random forces is varied from 0.0 to 0.75 to investigate the effect of the correlations between the uncertain loadings on the final topology.

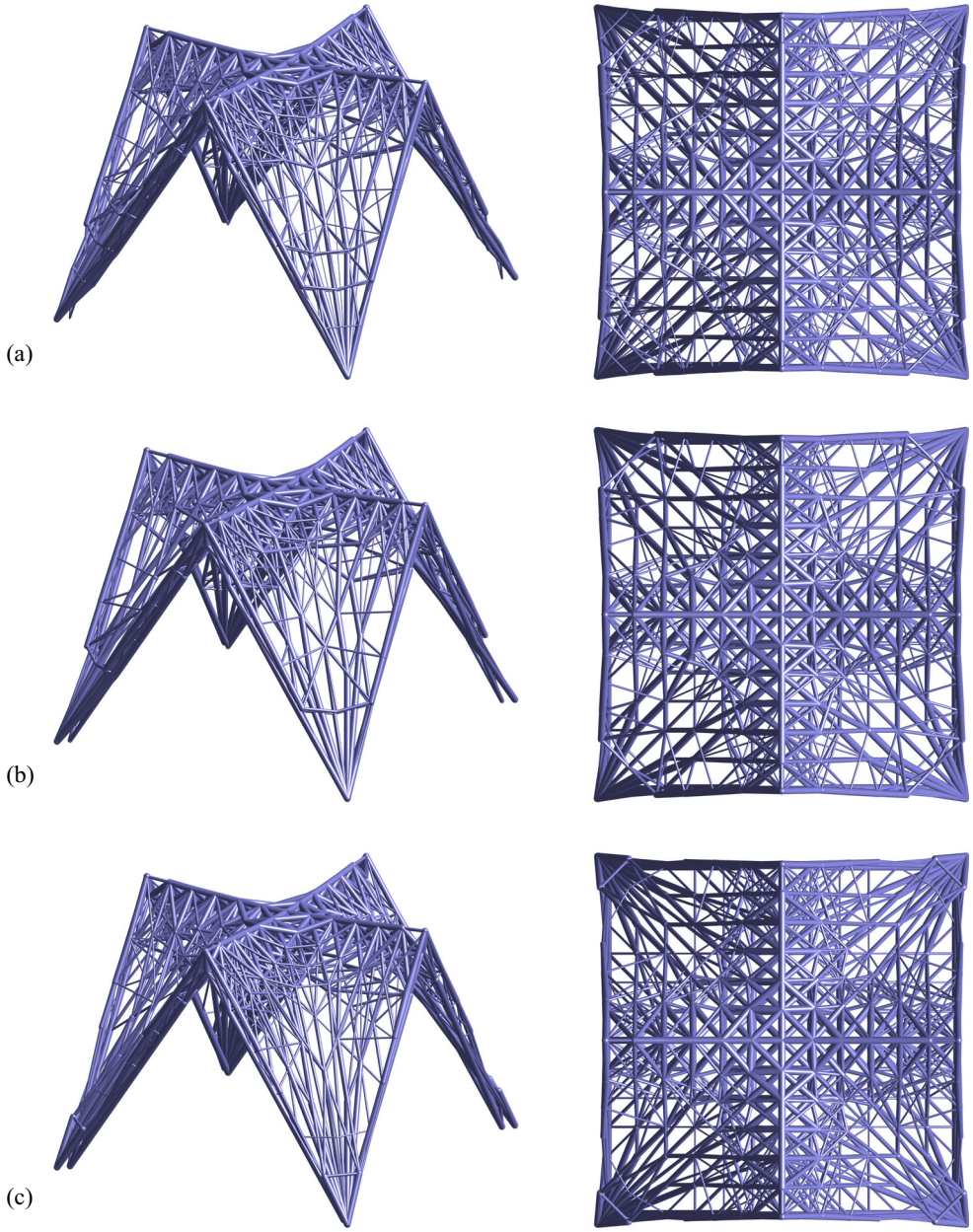

Fig. 23 Final topology by discrete filter (level 4 connectivity, $P_f^{\text{target}} = 0.0025$): **a** $\alpha_f = 0.02$, **b** $\alpha_f = 0.03$, and **c** $\alpha_f = 0.04$

The optimization results from DTO and RBTO are shown in Fig. 17. The line thicknesses in the plots are normalized to the upper bound of the cross-sectional area, which is 4.0 m^2. Compared to the results from DTO, overall cross-sectional areas on top and bottom chords are increased in RBTO. Furthermore, additional connectivities of truss elements are clearly observed in the RBTO results. Those connectivities in RBTO increase the stiffness of the truss structure so that the compliance decreases to satisfy the target failure probability. Furthermore, optimization results from RBTO show that the increase in the correlation coefficient results in the higher optimized volume, primarily because the positive correlation between forces increases the chance of violating the limit-state function by a raised compliance. The convergence histories of the objective function and the failure probability over iterations are plotted in Fig. 18.

4.6 Roof structure optimization

Finally, our method is applied to a large space structure fixed on ground level to identify the optimal topology while achieving the desired reliability. The problem domain is discretized with solid elements as shown in Fig. 19a. Figure 19b, c provide top and side views,

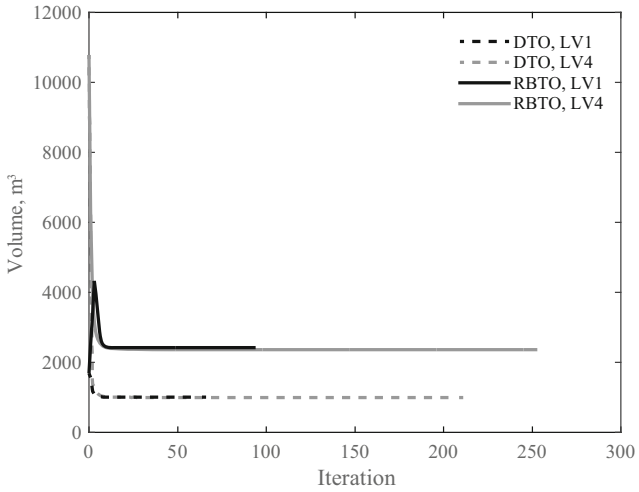

Fig. 24 Convergence history of roof structure optimization

respectively. Based on the discretized domain, the ground structure analysis and design in 3D (GRAND3, Zegard and Paulino 2015) were adopted to generate a ground structure using restriction zones (Fig. 20a, b). The restriction zones prevent truss members in the ground structure from passing through the restricted region. Two connectivity levels of the ground structure, shown in Fig. 20c, d, are generated and used for optimization while initial design variables are set to 0.25 m^2. Young's modulus and applied forces (Fig. 19a) are considered as random variables following normal distributions. The compliance under multiple loads is computed as

$$C(\mathbf{A},\mathbf{X}) = \sum_{i=1}^{n_f} \mathbf{f}_i^{\mathrm{T}}(\mathbf{X})\mathbf{u}_i(\mathbf{A},\mathbf{X}) \tag{23}$$

where n_f denotes the number of applied forces. Parameters of the probabilistic constraint on the compliance, and random variables, and the discrete filter are given in Table 7.

Figures 21 and 22 show a comparison of the optimized results for level 1 and 4 connectivity levels, respectively by DTO and RBTO. The connectivity level leads to the different topologies such as different connectivity of members in optimized solutions. Differences in optimal solutions between the deterministic and the probabilistic constraints can be clearly observed from the optimized results. To achieve the constraint on the failure probability, the overall member sizes are increased and more connectivities between bars remain. Figure 23 shows optimal topologies based on varying filter sizes. It should be noted that those solutions in global equilibrium satisfy the target failure probability. Finally, Fig. 24 shows the convergence histories of the volume in optimization. The resulting volume of high connectivity level is slightly reduced for both DTO and RBTO, as expected since a higher number of design variables (connectivities) typically reduce the objective function. Table 8 presents results associated with the roof structure optimization problem.

5 Concluding remarks

This paper presents a framework of single-loop reliability-based topology optimization that incorporates the discrete filtering scheme proposed by Ramos Jr. and Paulino (2016). Reliability-based topology optimization using the ground structure method with the conventional filtering scheme (cut-off) often leads to solutions that violate the prescribed failure probability after the post-processing. The proposed method successfully finds topology optimization solutions that satisfy the target failure probability and that are in global equilibrium. Numerical verifications by the first-order reliability method and Monte Carlo simulations confirm that the optimal topologies obtained by the proposed approach satisfy the given probabilistic constraints, unlike those by a conventional filtering scheme.

The effect of uncertainties in load and material property on optimal topologies are observed and investigated through comparison with the results of deterministic optimization. Using the discrete filter parameter and the connectivity level of the ground structure results in the various topologies with different optimized sizes while satisfying the desired failure probability. The variety of optimal solutions obtained from the proposed method can allow engineers to develop multiple structural design schemes.

In the present study, a single probabilistic constraint on the compliance is considered. In reality, different types of constraints such as displacement constraints and stress constraints under uncertainties are also of great interest in structural engineering. Most truss structures are indeterminate so that single failure (or a

Table 8 Representative parameters for optimal solutions of the roof structure problem

	Level 1 connectivity	Level 4 connectivity			
	Filter size, α_f				
	0.01	0.01	0.02	0.03	0.04
Volume	2,419.73	2,361.73	2,376.27	2,433.11	2,531.09
$\|\|\mathbf{Ku-f}\|\|/\|\|\mathbf{f}\|\|$	3.10×10^{-6}	2.57×10^{-6}	2.69×10^{-6}	3.40×10^{-5}	2.69×10^{-5}
P_{FORM}	0.0025	0.0025	0.0025	0.0025	0.0025

component) may not result in failure of the entire structural system. Therefore, the aforementioned failure events and various failure sequences need to be considered for more realistic applications of engineering designs. Moreover, a system failure event with statistical dependence between component failure events needs to be addressed in RBTO. Those remain as potential future research topics.

Funding information The authors gratefully acknowledge funding provided by the National Science Foundation (NSF) through projects 1234243 and 1663244. We also acknowledge support from the Raymond Allen Jones Chair at the Georgia Institute of Technology. The third author acknowledges the support from the Institute of Construction and Environmental Engineering at Seoul National University, and the National Research Foundation of Korea (NRF) Grant (No. 2015R1A5A7037372), funded by the Korean Government (MSIP).

Compliance with ethical standards

Conflict of interest The authors declare that they have no conflict of interest.

References

Ba-abbad M, Nikolaidis E, Kapania R (2006) A new approach for system reliability-based design optimization. AIAA J 44(5):1087–1096

Bendsøe MP, Sigmund O (2003) Topology optimization—theory, methods and applications, 2nd edn. Engineering Online Library. Springer, Berlin

Bobby S, Spence SM, Bernardini E, Kareem A (2014) Performance based topology optimization for wind-excited tall buildings: a framework. Eng Struct 74:242–255

Christensen PW, Klarbring A (2009) An introduction to structural optimization. Springer, Linköping

Chun J, Song J, Paulino GH (2016) Structural topology optimization under constraints on instantaneous failure probability. Struct Multidiscip Optim 53(4):773–799

Deaton J, Grandhi R (2014) A survey of structural and multidisciplinary continuum topology optimization: post 2000. Struct Multidiscip Optim 49(1):1–38

Der Kiureghian, A. (2005). First- and second-order reliability methods. Chapter 14 in Engineering design reliability handbook, E. Nikolaidis, D. M. Ghiocel and S. Singhal, Edts., CRC Press, Boca Raton, FL

Descamps B, Filomeno Coelho R (2014) The nominal force method for truss geometry and topology optimization incorporating stability considerations. Int J Solids Struct 51(13):2390–2399

Du XP, Chen W (2004) Sequential optimization and reliability assessment method for efficient probabilistic design. J Mech Des 126(2):225–233

Enevoldsen I, Sorensen JD (1994) Reliability-based optimization in structural engineering. Struct Saf 15(3):169–196

Frangopol DM, Maute K (2005) Reliability-based optimization of civil and aerospace structural systems. In: Engineering Design Reliability Handbook. CRC, Boca Raton, FL Chap. 24

Groenwold AA, Etman LFP (2008) On the equivalence of optimality criterion and sequential approximate optimization methods in the classical topology layout problem. Int J Numer Methods Eng 73(3):297–316

Guest JK, Igusa T (2008) Structural optimization under uncertain loads and nodal locations. Comput Methods Appl Mech Eng 198(1):116–124

Guo X, Cheng GD, Olhoff N (2005) Optimum design of truss topology under buckling constraints. Struct Multidiscip Optim 30(3):169–180

Guo X, Bai W, Zhang W (2009a) Confidence extremal structural response analysis of truss structures under static load uncertainty via SDP relaxation. Comput Struct 87(3–4):246–253

Guo X, Bai W, Zhang W, Gao X (2009b) Confidence structural robust design and optimization under stiffness and load uncertainties. Comput Methods Appl Mech Eng 198(41–44):3378–3399

Guo X, Du J, Gao X (2011) Confidence structural robust optimization by non-linear semidefinite programming-based single-level formulation. Int J Numer Methods Eng 86(8):953–974

Hemp W (1973) Optimum structures. Oxford University Press, Oxford

Jalalpour M, Guest JK, Igusa T (2013) Reliability-based topology optimization of trusses with stochastic stiffness. Struct Saf 43:41–49

Jin P, De-yu W (2006) Topology optimization of truss structure with fundamental frequency and frequency domain dynamic response constraints. Acta Mechanica Solida Sinica 19(3):231–240

Liang J, Mourelatos Z, Tu J (2004) A single-loop method for reliability-based design optimization. Proceedings of the ASME Design Engineering Technical Conferences

Liang J, Mourelatos ZP, Nikolaidis E (2007) A single-loop approach for system reliability-based design optimization. J Mech Des 129(12):1215–1224

Liang J, Mourelatos ZP, Tu J (2008) A single-loop method for reliability-based design optimisation. Int J Product Dev 5(1–2):76–92

Maute K, Frangopol DM (2003) Reliability-based design of MEMS mechanisms by topology optimization. Comput Struct 81(8–11):813–824

Mijar AR, Swan CC, Arora JS, Kosaka I (1998) Continuum topology optimization for concept design of frame bracing systems. J Struct Eng 124:541–550

Mitjana F, Cafieri S, Bugarin F, Gogu C, Castanie F (2018) Optimization of structures under buckling constraints using frame elements. Eng Optim:1–20

Nguyen T (2010) System reliability-based design and multiresolution topology optimization. Ph.D. thesis. Urbana-Champaign: University of Illinois

Nguyen TH, Song J, Paulino GH (2011) Single-loop system reliability-based topology optimization considering statistical dependence between limit-states. Struct Multidiscip Optim 44(5):593–611

Ohsaki M (2010) Optimization of finite dimensional structures. CRC Press

Ramos Jr. AS, Paulino GH (2016) Filtering structures out of ground structures—a discrete filtering tool for structural design optimization. Struct Multidiscip Optim 54(1):95–116

Royset JO, Der Kiureghian A, Polak E (2001) Reliability-based optimal design of series structural systems. J Eng Mech 127(6):607–614

Rozvany GIN (2008) Exact analytical solutions for benchmark problems in probabilistic topology optimization. EngOpt 2008–International Conference on Engineering Optimization, Rio de Janeiro

Rozvany GIN (2009) A critical review of established methods of structural topology optimization. Struct Multidiscip Optim 37(3):217–237

Shan S, Wang GG (2008) Reliable design space and complete single-loop reliability-based design optimization. Reliab Eng Syst Saf 93(8):1218–1230

Song J, Kang WH (2009) System reliability and sensitivity under statistical dependence by matrix-based system reliability method. Struct Saf 31(2):148–156

Stromberg LL, Beghini A, Baker WF, Paulino GH (2012) Topology optimization for braced frames: combining continuum and beam/column elements. Eng Struct 37:106–124

Talischi C, Paulino GH, Pereira A, Menezes IFM (2012) PolyMesher: a general-purpose mesh generator for polygonal elements written in MATLAB. Struct Multidiscip Optim 45(3):309–328

Tsompanakis Y, Lagaros ND, Papadrakakis M (2008) Structural design optimization considering uncertainties. Taylor & Francis, London

Tu J, Choi KK, Park YH (1999) A new study on reliability based design optimization. J Mech Des 121(4):557–564

Tyas A, Gilbert M, Pritchard T (2006) Practical plastic layout optimization of trusses incorporating stability considerations. Comput Struct 84(3–4):115–126

Zegard T, Paulino GH (2014) GRAND—ground structure based topology optimization for arbitrary 2D domains using MATLAB. Struct Multidiscip Optim 50(5):861–882

Zegard T, Paulino GH (2015) GRAND3—ground structure based topology optimization for arbitrary 3D domains using MATLAB. Struct Multidiscip Optim 52(6):1161–1184

Publisher's note Springer Nature remains neutral with regard to jurisdictional claims in published maps and institutional affiliations.